energies

MDPI

Review

Recent Advances in Ammonia Combustion Technology in Thermal Power Generation System for Carbon Emission Reduction

Hookyung Lee and Min-Jung Lee *

Energy Efficiency Research Division, Korea Institute of Energy Research, Daejeon 34129, Korea; hk.lee@kier.re.kr
* Correspondence: mjlee@kier.re.kr; Tel.: +82-42-860-3318

Abstract: With the formation of an international carbon-neutral framework, interest in reducing greenhouse gas emissions is increasing. Ammonia is a carbon-free fuel that can be directly combusted with the role of an effective hydrogen energy carrier, and its application range is expanding. In particular, as research results applied to power generation systems such as gas turbines and coal-fired power plants have been reported, the technology to use them is gradually being advanced. In the present study, starting with a fundamental combustion research case conducted to use ammonia as a fuel, the application research case for gas turbines and coal-fired power plants was analyzed. Finally, we report the results of the ammonia-air burning flame and pulverized coal-ammonia-air co-fired research conducted at the authors' research institute.

Keywords: carbon-neutral; carbon-free fuel; ammonia; combustion; gas turbine; coal-fired boiler

Citation: Lee, H.; Lee, M. Recent Advances in Ammonia Combustion Technology in Thermal Power Generation System for Carbon Emission Reduction. *Energies* **2021**, *14*, 5604. https://doi.org/10.3390/en14185604

Academic Editor: Ali Turan

Received: 12 July 2021
Accepted: 4 September 2021
Published: 7 September 2021

1. Introduction

Energy is a driving force for national industrial development and economic growth, and for the affluent life of people, and its consumption inevitably increases continuously. Humans have led economic and industrial development by using hydrocarbon-based fossil fuels such as coal and petroleum, and they are prevalent in developing countries. As the severity of the climate change problem increased about 150 countries agreed to co-operate and a climate change agreement was adopted at the Rio Environmental Conference in June 1992, and the Kyoto Protocol in 1996 to solve the global warming problem in earnest. This gradually expanded and led to the international treaty of the Paris Agreement in 2015, and governments were advised to submit long-term low greenhouse gas emission development strategies to the international community by 2020 in accordance with the Paris Agreement. At the same time, each country had declared that it will achieve carbon neutrality by 2050 or at the longest by 2060. Most of them set the target for 2050 because the Intergovernmental Panel on Climate Change (IPCC) suggested to limit the increase in global average temperature to 1.5 °C by 2100. This is because it suggested a path that global carbon dioxide emissions should be reduced by at least 45% compared to 2010 by 2030, and that carbon-neutrality should be achieved by 2050. Therefore, in line with the Paris Agreement's guidelines, and the goal of limiting the increase in global average temperature to 1.5 °C or less, most countries aim to reduce greenhouse gas emissions from human activities to the fullest extent; to absorb and remove emitted carbon, and bring the actual emissions to zero. Achieving carbon neutrality is a very challenging goal; however, the international community is demanding a higher achievement. Further details on this are contained in the biennial update reports, and COP26 will be held in the UK to discuss the latest developments [1]. To realize greenhouse gas reduction through innovation in the face of tightening environmental regulations, the development and early commercialization of prospective energy technology and investment to support them are emphasized.

The Netherlands Environmental Assessment Organization estimates that the world emitted 57.4 Gt CO_2eq greenhouse gases in 2019 [2]. Among them, global energy-related

carbon dioxide (CO_2) emissions are 33.4 Gt CO_2eq. This amount is also consistent with that reported by the IEA [3]. The continuous increase of CO_2 in the atmosphere is mainly driven by fossil fuel combustion and calcination of carbonates. The dominant drivers of CO_2 are the combustion of coal, oil, and natural gas, representing 89% of global CO_2 emissions, with respective shares of 39%, 31%, and 18%. In particular, the combustion of fuel in thermal power plants is a major cause of large-scale CO_2 generation and accounts for the dominant proportion of the electricity generation sector. In the field, coal, a solid fuel, is mainly used in coal-fired power plants, and gaseous fuels such as natural gas are mainly used in combined cycle power plants, including gas turbines.

The dominance of greenhouse gas emissions from fossil fuel combustion has already been well demonstrated in existing analysis data, and associated researchers in the fields of combustion, energy, and the environment are well aware of this fact. Therefore, it is unnecessary to say that innovative development of fuel combustion technology is needed to meet the future carbon-neutral system goals. However, the innovation in energy conversion is being promoted more rapidly than in the past, and intensive R&D activities are needed to support this technology. Although global R&D activities to move towards a renewable and hydrogen society are mainly centered on transportation and fuel cells, there are still many goals to be achieved for the full-cycle, large-scale practical use of hydrogen production, transport, supply, and utilization for commercialization. As it has been consistently mentioned in the past, it will take a long time as well a huge socio-economic investment for the government and private sector to establish an infrastructure for the supply of hydrogen.

Therefore, to implement the rapidly changing carbon emission reduction regulations and fulfill the promises made with the international community, technologies that are relatively easy to commercialize need to be implemented. Methods for reducing greenhouse gases include improving the thermal system efficiency and capturing CO_2 through downstream facilities. However, it would be economical in terms of post-treatment cost if the combustion stage uses a fuel that does not emit carbon from the source. The cost of producing a carbon-free fuel and the CO_2 footprint must be considered together. Ammonia (NH_3) is expected to be a carbon-free fuel. To realize a carbon-neutral society in 2050, for example, Japan has presented an action plan for 14 important areas that are expected to grow in the future as a greenhouse gas reduction industry in terms of growth strategies. In particular, they emphasized that ammonia is an effective fuel when combusted with pulverized coal in a coal-fired boiler. In addition, R&D was conducted to apply fuel ammonia to coal-fired power plants, gas turbine combustion, and industrial furnace combustion through the cross-ministerial strategic innovation promotion program (SIP) project from 2014 to 2018 [4]. Through this project, the technical feasibility of using fuel ammonia has been verified, and research is underway with the goal of commercializing the related technology through the new energy and industrial technology development organization (NEDO) project, a follow-up task [5]. Because the advantages (carbon-free fuel) and disadvantages (low reactivity and fuel-NOx production) of using ammonia as a fuel clearly exist, research has been conducted to overcome these technical bottlenecks and supply problems, and some of the results linked to demonstrations show the effect of reducing greenhouse gas emissions [6–9].

Ammonia was first studied as an alternative fuel for internal combustion engines rather than for reducing greenhouse gas emissions. As available resources became scarce due to World War II, interest was drawn in fuels other than fossil fuels, and accordingly, the possibility of using ammonia as a fuel drew attention [10–16]. The technology of using ammonia as a fuel in automobile internal combustion engines has been used for trucks in Norway since the 1930s, and was developed in Belgium in 1943 [17]. In the 2000s, there was a research case of a compression ignition engine to which a mixed combustion system of ammonia-diesel and ammonia-DME fuel was applied [18,19]. The optimal ammonia co-firing rate was 60%, and when it was lower than this, the flame temperature decreased and the amount of NOx produced decreased compared to when only diesel fuel was used. However, as the ammonia ratio increased, the amount of NOx produced due to nitrogen

contained in the fuel increased sharply. Currently, research is underway to apply ammonia to spark-ignition engines [20,21]. In addition, there are quite a lot of research results aimed at overcoming the challenge of its low reactivity, and most of the results have proposed to achieve this by blending ammonia with a high-reactivity fuel [22,23]. Regarding the production of prototype vehicles using ammonia as fuel, in 2007, the University of Michigan developed an ammonia-gasoline combustion engine and operated it from Detroit to San Francisco [24]. In 2013, the Korea Institute of Energy Research developed an ammonia-gasoline engine, called AmVeh, by remodeling a gasoline-LPG fueled engine [25]. Recently, the development of fuel-powered ships utilizing LNG, hydrogen, and ammonia for low-carbon emissions has been notable [26,27]. Ammonia-fueled propulsion ship development plans are being reported mainly by companies [28–32]. In addition, research on the concept of a marine engine for hydrogen-ammonia co-firing is in progress [33–35]. Kim et al. conducted environmental and economic assessments associated with an alternative ship propulsion system fueled by ammonia [36]. Technologies capable of emitting greenhouse gases from the operational aspects of ships were reviewed by Bouman et al. [37].

In the field of thermal power generation that we discuss in this study, the combustion characteristics of ammonia and their application to gas turbines and coal-fired boilers are being studied mainly in Japan, the United Kingdom, and Korea. Looking at what these countries have in common, they are surrounded by sea rather than connected to other countries (South Korea is a militarily divided country) and continents, and are characterized by high energy-use intensity. To achieve hydrogen economy and a carbon-neutral society, it is necessary to increase the production and use of hydrogen fuel. It is well known that hydrogen is produced by processes such as reforming and water electrolysis, unlike fuels mined in nature [38–42]. However, there is a limit to the amount of hydrogen that can be produced in these countries. It is necessary to supplement it by shipping from other countries with abundant renewable energy for the introduction of green-hydrogen that does not emit CO_2 during the water electrolysis process using solar power or blue-hydrogen by the reforming process with carbon capture and storage (CCS) facilities. Therefore, it is necessary to develop a material that can act as a carrier for hydrogen, and ammonia has been considered the most appropriate material [43–45]. There are also a number of studies comparing the transport mediums of hydrogen [46–53]. Hydrogen can be produced by cracking ammonia; however, ammonia itself is a combustible material with a calorific value and can be used as a fuel in a thermal system. Therefore, ammonia could be used directly as a fuel, and combustion characteristics were studied because the ammonia-cracking process required another energy source. This also has the advantage that the unit cost of ammonia is much lower than that of hydrogen [43–45].

Figure 1 shows the CO_2-free ammonia value chain used in a direct combustion system through the transport process after the green-hydrogen, produced through the water electrolysis process using renewable energy, and the blue-hydrogen, through the fossil fuel reforming process with CCS, are synthesized into ammonia. The current large-scale ammonia production is achieved by the Haber-Bosch process. In the future, the power used to maintain the operating conditions in the Haber-Bosch process must also be produced from renewable energy sources to achieve a truly carbon-neutral system [54].

In the present study, the recent R&D trends associated with gas turbines and coal-fired boilers using fuel ammonia are summarized by presenting the application results for demonstration. The experimental research results of the institutions that have been investigating fundamental combustion characteristics for a long time are summarized for the development of such commercial facilities. Finally, the brief research results of the Korea Institute of Energy Research, which is leading the ammonia combustion technology in Korea, are reported.

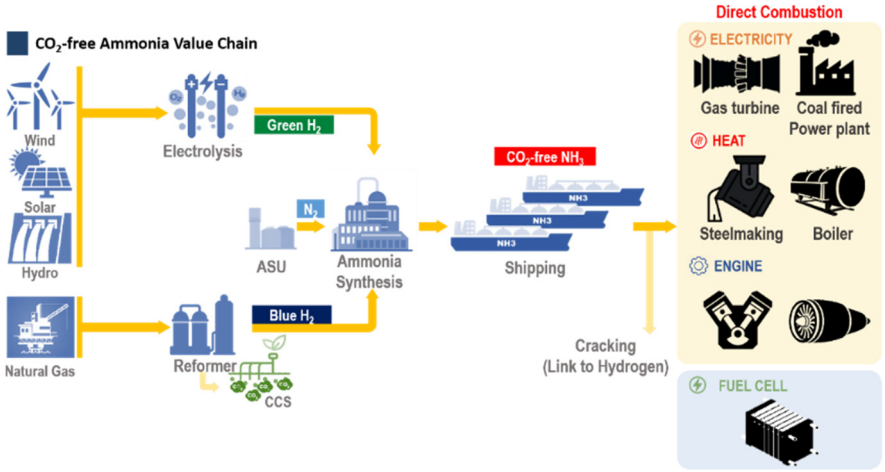

Figure 1. A schematic flow on CO_2-free ammonia value chain.

2. Researches on Fundamental Combustion Characteristics of Fuel Ammonia

An important challenge to overcome for the direct use of ammonia as a fuel is its low reactivity and high NOx production [55–57]. The low reactivity is due to the low laminar flame burning velocity, flame temperature, and flammability limit compared to conventional hydrocarbon fuels. The high NOx production is due to the fuel-NOx mechanism, which has a higher reaction rate at a lower temperature than conventional thermal-NOx. Therefore, to maximize the advantage of ammonia, which is a carbon-free fuel, these two disadvantages must be overcome. Although basic combustion studies are complementary, they can be broadly divided into laminar and turbulent flame studies. Laminar flame studies focus on combustion rate, ignition energy, flammability limit, and ignition delay time, whereas turbulent flame studies concentrate on flame stabilization characteristics in turbulent fields. In addition, based on the combustion experimental results of ammonia-air and mixed fuels such as ammonia-hydrogen-methane under laminar and turbulent flow conditions, the existing reaction mechanism is modified or improved for the accuracy of ignition delay and NOx composition in a high-pressure environment. As the study on the mechanism of ammonia combustion is an early one, it is necessary to compare and verify various mechanisms according to combustion conditions before use.

2.1. Apparent Observation on Ammonia Flame

Even though the thermodynamic properties of ammonia are similar to those of propane, its calorific value per unit mass is lower than that of other fuels, and its auto-ignition temperature is higher than that of other fuels. Table 1 shows the thermal properties and fundamental combustion characteristics of ammonia and other hydrocarbon fuels [55].

Table 1. Thermodynamic characteristics of ammonia and other hydrocarbon fuels [55].

	NH_3	H_2	CH_4	C_3H_8
Boiling temperature at 1 atm [°C]	−33.4	−253	−161	−42.1
Condensation pressure at 25 °C [atm]	9.9	n/a	n/a	9.4
Lower heating value [MJ/kg]	18.6	120	50	46.4
Flammability limit [Equivalence ratio]	0.63–1.4	0.1–7.1	0.5–1.7	0.51–2.5
Adiabatic flame temperature [°C]	1800	2110	1950	2000
Maximum laminar burning velocity [m/s]	0.07	2.91	0.37	0.43
Minimum auto ignition temperature [°C]	650	520	630	450

As shown in Figures 2 and 3, in the case of methane, a blue flame is formed by high-temperature luminescence of CH*, whereas in ammonia, a yellow or orange flame is observed by NH_2* and superheated H_2O vapor [58,59]. Hayakawa et al. investigated

through flame self-luminescence spectra that the NH_2 concentration rapidly increased under fuel-rich conditions, resulting in a darker color.

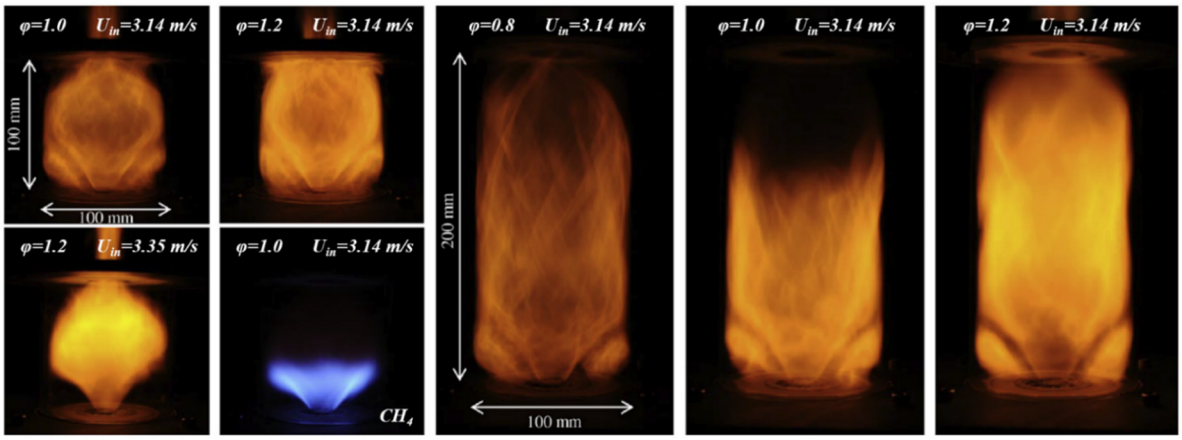

Figure 2. NH_3-air and CH_4-air flames stabilized in the swirl burner with cylindrical liners. Modified from [58]. Courtesy of Elsevier [58].

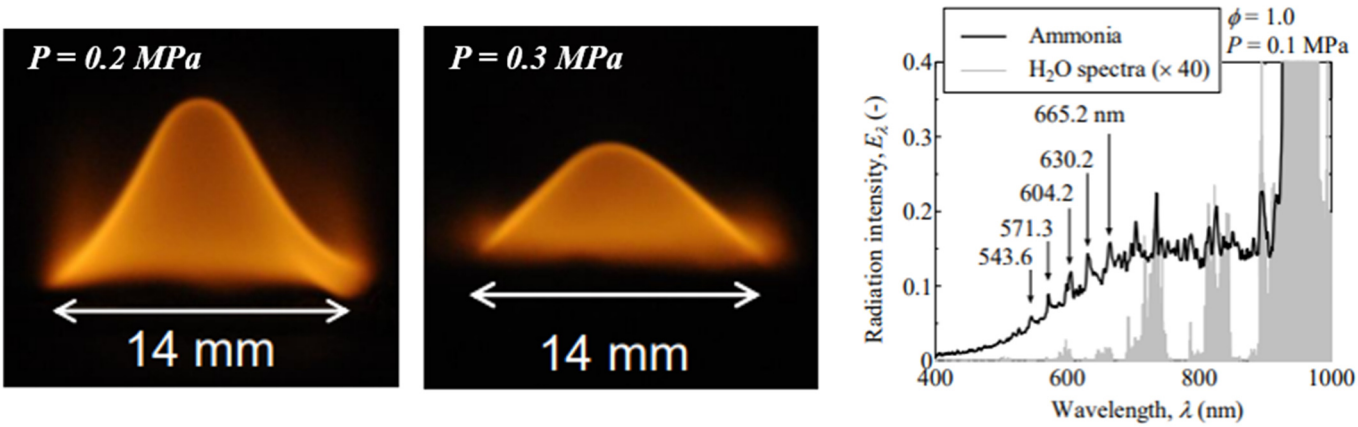

(**a**) NH_3-air flame images (**b**) Radiation intensity and wavelength

Figure 3. NH_3-air flames stabilized on the nozzle-type burner and radiation intensity analysis: (**a**) Images of NH_3-air premixed flame at stoichiometric condition; (**b**) Relationship between radiation intensity, E_λ, and wavelength, λ, of $\varphi = 1.0$ at $p = 0.1$ MPa. Modified from [59]. Courtesy of the Japan Society of Mechanical Engineers [59].

In addition, it can be seen that ammonia, which shows a relatively longer flame than methane under the same conditions, has a very low combustion rate compared to methane, and it can be predicted that the radiative heat transfer characteristics are also changed due to different wavelengths emitted from the flame.

2.2. Laminar Reacting Flow of Ammonia Flame

The most important combustion characteristic in combustor design is the laminar flame burning velocity. Figures 4 and 5 indicate the experimental results of spherical flame propagation [55,60]. Similar to the hydrogen flame, the equivalence ratio condition having the highest burning velocity is biased toward the fuel-rich condition. This is a result of the preferential diffusion of hydrogen molecules dissociated from ammonia at high temperature, and the burning velocity is up to 7 cm/s under the condition of an equivalence ratio of 1.1, which corresponds to 20% of the CH_4-air burning velocity. Therefore, it can be seen that the measurement range of the burning velocity using the spherical propagation flame of ammonia-air combustion is approximately 0.7 to 1.25 of the equivalence ratio,

which is slightly lower than the flammability limit of 0.63 to 1.4 suggested by NIST, as indicated in Table 1.

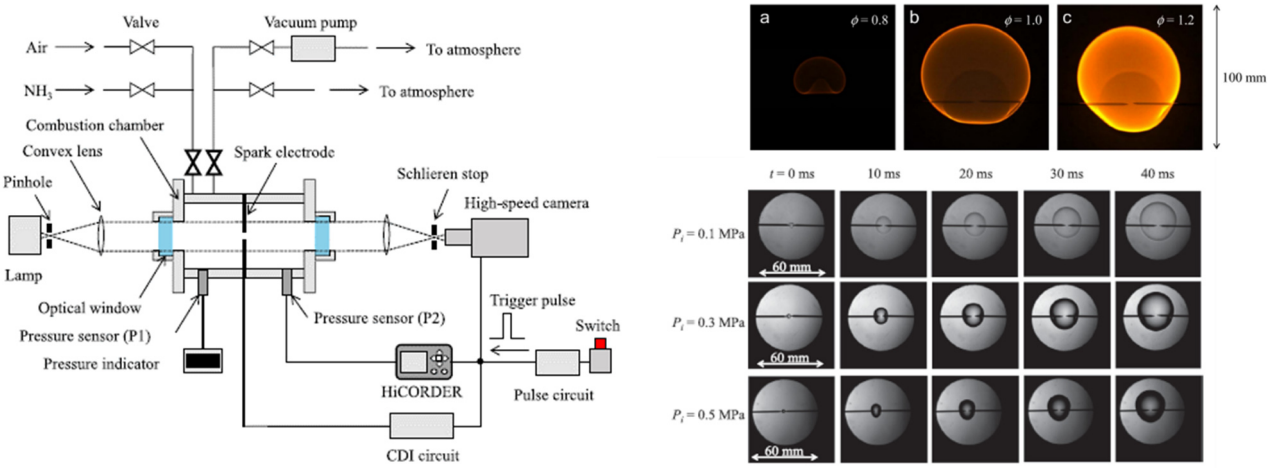

(**a**) Schematic of experimental setup (**b**) Direct and Schlieren images

Figure 4. Experimental apparatus and results for measuring spherical flame propagation: (**a**) Schematic of experimental setup; (**b**) Direct and Schlieren images of NH_3-air flame. Modified from [60]. Courtesy of Elsevier [60].

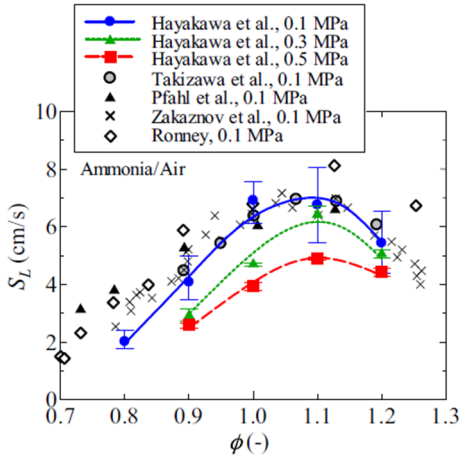

Figure 5. Experimental and numerical results of the relationship between unstretched laminar burning velocity, S_L, and equivalence ratio, φ. Courtesy of Elsevier [55].

In general, when measuring the burning velocity using a spherical propagation flame, the change in the flame radius over time was measured, and the burning velocity according to the strain rate was derived from the change in the flame curvature and subsequently the laminar burning velocity is calculated in the unstretched condition. In this case, the sensitivity (slope) of the burning rate according to the strain rate is generally expressed as the Markstein length or the Markstein number divided by the thickness of the flame zone. In general, when the Markstein number is negative, an unstable flame could be observed, and a stable flame for a positive value. However, depending on the degree of thermal-diffusive instability, if the Markstein number is a relatively low positive number, cellular instability may occur. Ammonia has a Lewis number lower than 1 under fuel-lean conditions similar to CH_4-air and H_2-air flames, and the Markstein number is negative number under conditions below an equivalence ratio of 0.9. In addition, the Markstein number is further reduced with increasing pressure, and there is a possibility that flame instability due to thermal-diffusive instability is strengthened under the same equivalence ratio.

As shown in Figure 6, the burning velocity decreased with an increase in pressure. As the experimental results under high-pressure conditions are still lacking, it is considered that additional experiments are needed to design a combustor operating at 10 bar or higher.

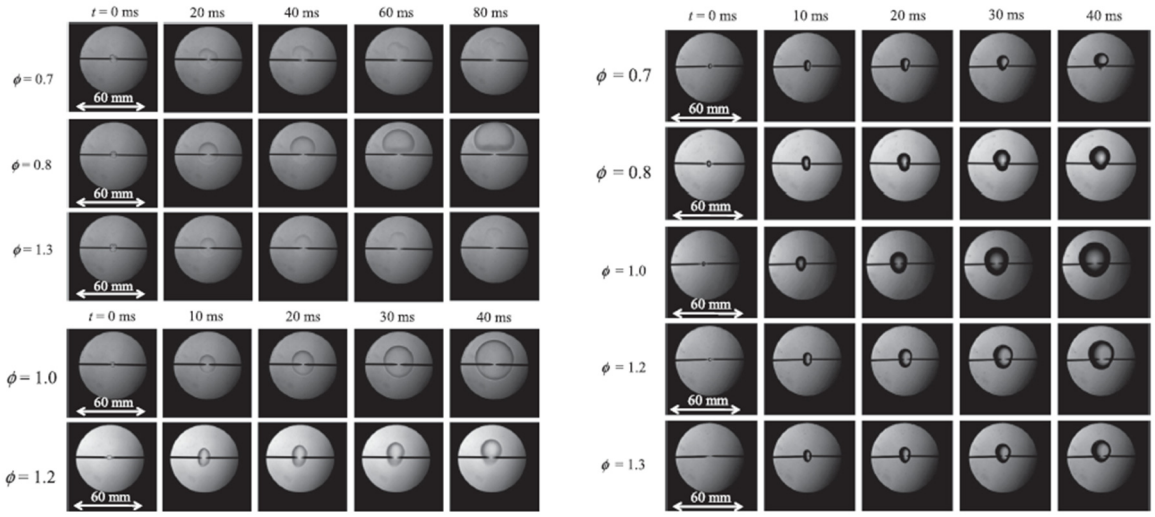

(**a**) Schlieren images at 0.1 MPa (**b**) Schlieren images at 0.5 MPa

Figure 6. Schlieren images of NH_3-air premixed flames: (**a**) P_i = 0.1 MPa; (**b**) P_i = 0.5 MPa. Courtesy of Elsevier [60].

2.3. Turbulent Reacting Flow of Ammonia Flame

As the flame forms a turbulent field inside a practical combustor, it is very important to understand the turbulent combustion characteristics. The flame formed by turbulent flow expands as it corrugates or warps. At this time, the flame can be extinguished by excessive strain rate due to the local unsteady velocity gradient. Fundamental research on turbulent flames of pure ammonia-air combustion has less information than laminar flow studies. Ichimura et al. conducted experiments on the stabilization region of ammonia-air flames under turbulent flow conditions by controlling the fan rotation speed in a static chamber, as shown in Figure 7 [61].

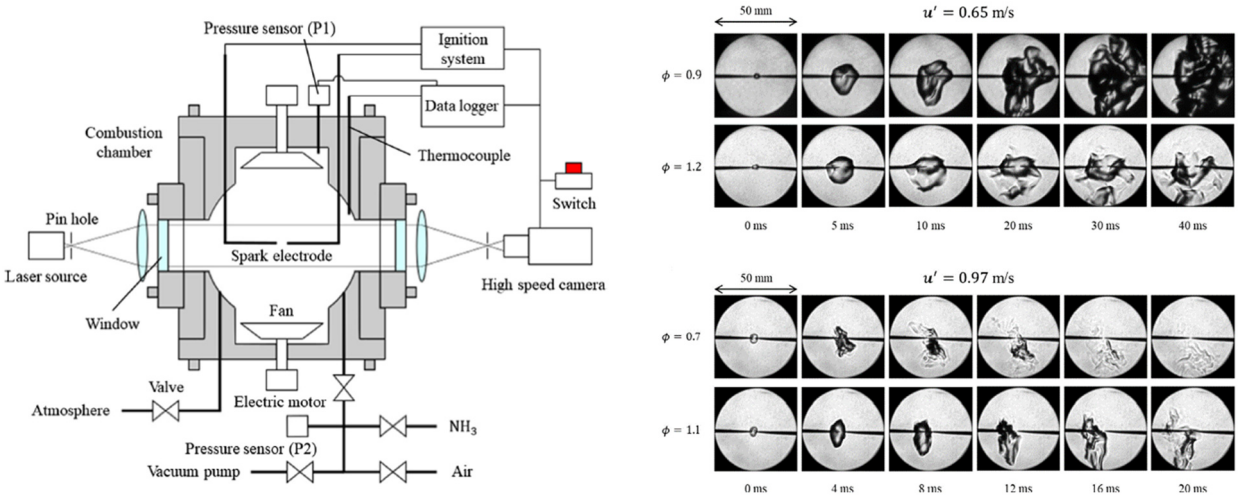

(**a**) Schematic of experimental apparatus (**b**) Schlieren images of flame

Figure 7. Experimental apparatus and results to investigate NH_3-air combustion characteristics in a turbulent field: (**a**) Schematic of experimental apparatus; (**b**) Schlieren images of NH_3-air mixture flame at each equivalence ratio and turbulence intensity. Courtesy of Elsevier [61].

The turbulence intensity according to the rotational speed of the fan was measured using particle image velocimetry (PIV) to confirm linearity. In the experiment, the Karlovitz number at the time of flame extinguishing was derived while increasing the turbulence intensity under the same equivalence ratio condition. The larger the Karlovitz number, longer the chemical reaction characteristic time, and the relatively shorter flow characteristic time due to the velocity fluctuation component in the turbulent flow field, that is, the turbulence intensity.

As shown in Figure 8, the stabilization region of the ammonia-air flame under the turbulence condition has the widest range when the equivalence ratio is 0.9, indicating that the resistance to high turbulence intensity is the highest at this ratio. The reason why the flame stabilization region is widened at 0.9 instead of 1.1, which has the maximum laminar burning velocity of ammonia-air combustion, is explained by the Markstein number in the turbulent flow field. In the case of an ammonia-air flame, it has a negative Markstein number in the fuel-lean condition, and the burning velocity increases due to thermal-diffusive instability from stretching. Therefore, the turbulent flame stabilization area can be determined by the flame strain rate effect, thermal-diffusive instability, and the Markstein number according to the increase in turbulence intensity.

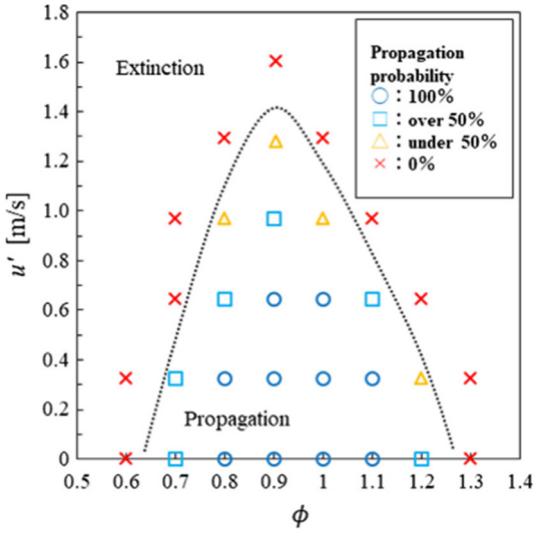

Figure 8. Flame propagation probability map of the NH_3-air flames at the turbulence intensity. Courtesy of Elsevier [61].

2.4. Effect of Ammonia-Hydrogen and -Methane Mixture on the Combustion Characteristics

As mentioned earlier, the burning velocity of ammonia-air flames is very low compared to that of other fuels, up to 7 cm/s. From a practical point of view, various methods can be considered to overcome the low burning velocity. The combustion rate of fuel is proportional to the fuel consumption rate per unit mass, and a low value means that the time required for the chemical reaction is large. Therefore, in an environment with a low flow characteristic time, such as a turbulent flow field, the flame cannot be maintained or the flame stabilization range is narrowed. This is the reason why the length of the ammonia flame is relatively longer, as shown in Figure 2. Therefore, to widen the flame stabilization area and for high-load combustion in a relatively narrow space, it is necessary to increase the combustion rate of ammonia through an appropriate technique. Methods for increasing the combustion rate of ammonia include mixing with a fuel having a relatively high burning velocity, enriching oxygen, and preheating the fuel with an oxidizer. In terms of fuel mixing, the most studied method is to mix fuels such as hydrogen and methane in an appropriate ratio to be similar to general hydrocarbon fuels, and research to determine the combustion rate under oxygen-enriched conditions is also in progress.

Ichikawa et al. studied the change in burning velocity when hydrogen and methane were added to an ammonia-air flame [62,63]. The experimental equipment for hydrogen addition is as shown in Figure 4, and is at the level of adding a hydrogen supply line. As shown in Figure 9, it can be seen that the combustion rate increases up to 30 times depending on the hydrogen fraction of the mixed fuel. It is important to observe that when about 40% of hydrogen is mixed with ammonia, it has a burning rate of 40 cm/s, which is similar to the maximum value of the methane-air flame. In contrast, as the burning velocity decreases as the pressure increases, additional means are required to design a combustion operated machine under high pressure conditions, such as a gas turbine.

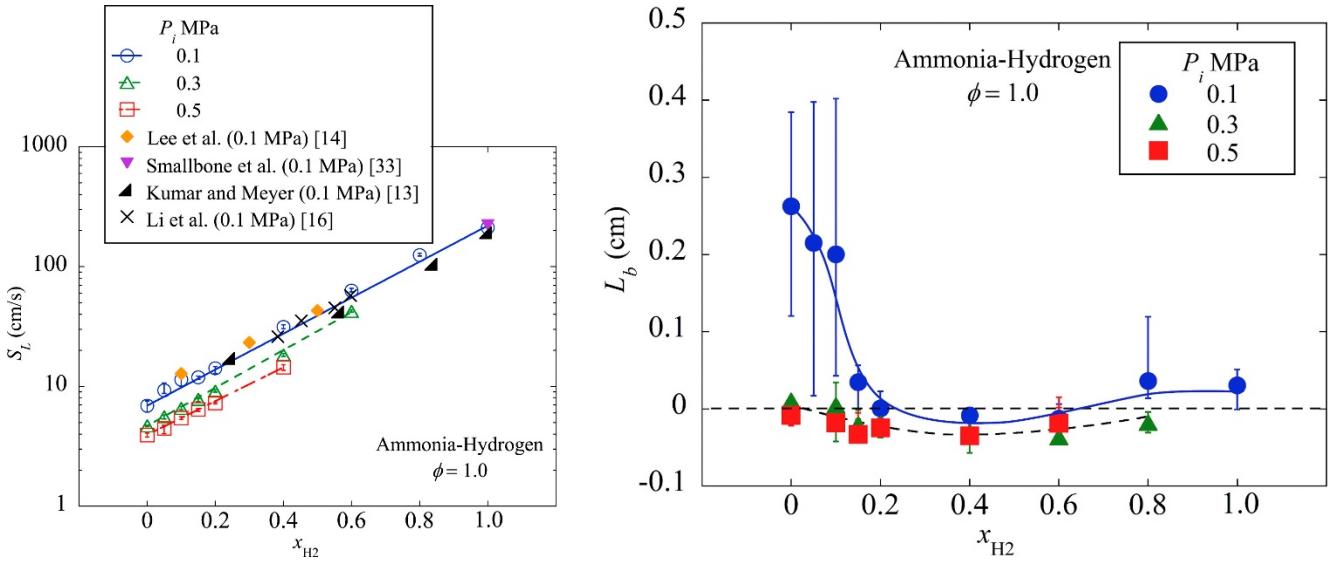

(**a**) Unstretched laminar burning velocity on different H_2 ratio

(**b**) Markstein length on different H_2 ratio

Figure 9. Burning velocity change due to H_2 addition to NH_3: (**a**) Relationship between unstretched laminar burning velocity, S_L, and hydrogen ratio, X_{H2}, in initial pressure varies from 0.1 to 0.5 MPa; (**b**) Relationship between the burned gas Markstein length, L_b, and the H_2 ratio, X_{H2}. Courtesy of Elsevier [62].

As shown in Figure 10, Ku et al. investigated the combustion characteristics of expanding spherical premixed methane-ammonia-air flames [64]. The premixed methane-ammonia-air flames produced less CO_2; however, the flames became thicker and propagated slower than the pure methane-air flames. When 20–40% of methane was replaced with ammonia, it was possible to reduce CO_2 emissions approximately by 25% with moderate reduction in laminar burning velocities. However, NOx increased because of the fuel-NOx mechanism, which was found to be more dominant than the potential NOx reduction with reduced flame temperature, resulting in the maximum values of the NOx mole fraction.

Lee et al. investigated the fundamental combustion characteristics of hydrogen-ammonia-air flames [65]. Specifically, the effects of partial ammonia co-firing on hydrogen-air flames were experimentally investigated. Ammonia is capable of reducing the flame temperatures and laminar burning velocities of hydrogen-air flames. In particular, the relative amount of decrease in laminar burning velocities with ammonia addition is more substantial for fuel-rich conditions. At fuel-rich conditions, the amount of NOx emissions increased and then decreased with ammonia addition and the increased amount of NOx and N_2O emission with ammonia addition is much lower than that under fuel-lean conditions. Figure 11 shows the shadowgraph images of ammonia-substituted hydrogen-air flames with various equivalence ratios. The laboratory additionally conducted a study on the combustion stability and NOx emission characteristics during hydrogen-ammonia co-firing [66,67].

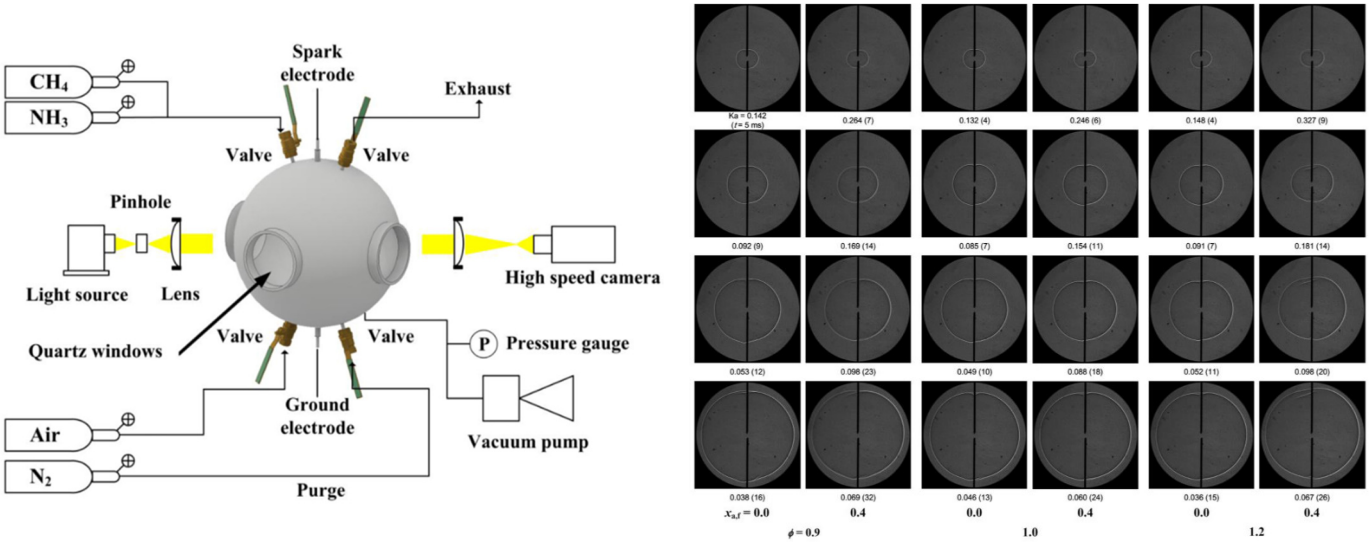

(**a**) Schematics of experimental apparatus (**b**) Shadowgraph images of CH_4-NH_3-air flames

Figure 10. Equipment and results for measurement of combustion characteristics of CH_4-NH_3-air flames according to NH_3 co-combustion ratio: (**a**) Schematics of experimental apparatus; (**b**) Shadowgraph images of premixed CH_4-NH_3-air flames at normal temperature and pressure. Courtesy of Elsevier [64].

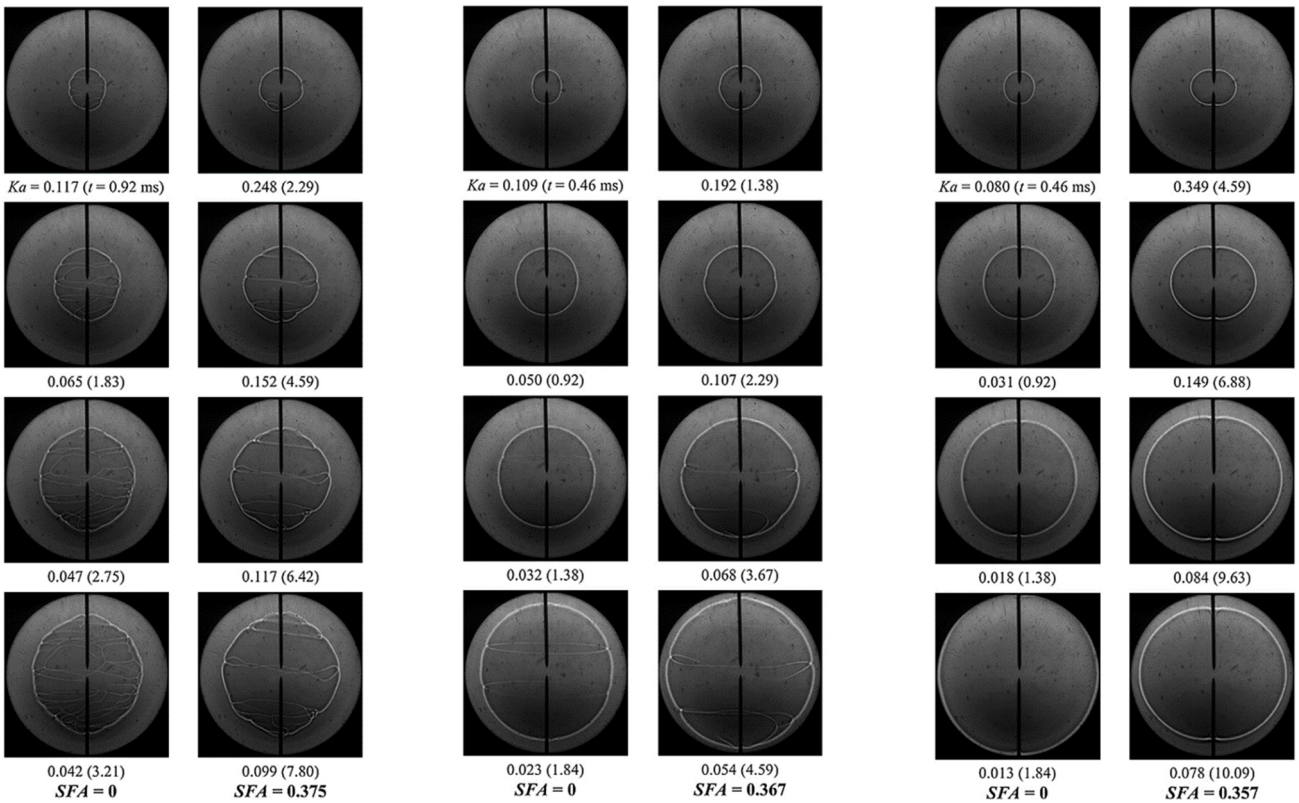

(**a**) φ = 0.6 (**b**) φ = 1.0 (**c**) φ = 1.67

Figure 11. Shadowgraph photographs of NH_3-substituted H_2-air flames. SFA means the volumetric fraction of H_2 replaced by NH_3: (**a**) φ = 0.6; (**b**) φ = 1.0; (**c**) φ = 1.67 at normal temperature and pressure. Courtesy of Elsevier [65].

Tang et al. investigated the laminar premixed flame of ammonia mixed with hydrogen and methane [68]. They found that hydrogen was an effective substitution for the combustion performance of ammonia fuel. The experimental results show that the ammonia-hydrogen flame has a smaller lower blowout limit and lean combustion rate, and

a higher rich combustion limit. Figure 12 shows the flame images and effects of equivalence ratio of ammonia-hydrogen and ammonia-methane on blowout limits of flames.

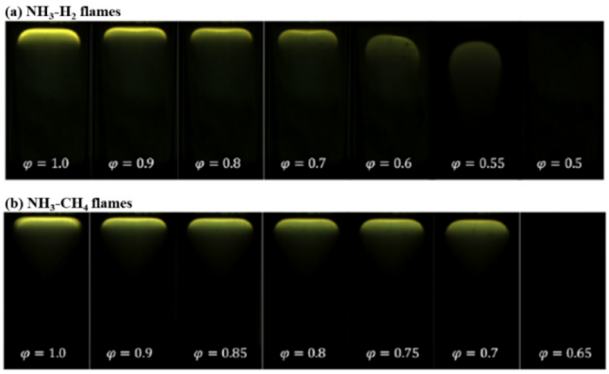

(**a**) Images of NH_3-H_2 and NH_3-CH_4 flames

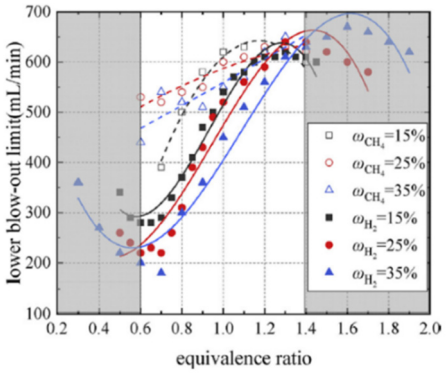

(**b**) Effects of equivalence ratio on lower blow-out limits of flames

Figure 12. Flame observation and effects of equivalence ratio on blowout limit: (**a**) NH_3-H_2 and NH_3-CH_4 flames extinguishing with decreasing equivalence ratio; (**b**) Blowout shape according to equivalence ratio on variable H_2 and CH_4 flow. Courtesy of Elsevier [68].

Zhang et al. investigated the effect of methane and hydrogen substitution on the emission characteristics of ammonia-air flame in a model gas turbine combustor [69]. The instantaneous OH profile and the global outlet emission were measured using planar laser-induced fluorescence (PLIF) and Fourier transform infrared (FTIR) spectroscopy, respectively. When the co-firing rate of hydrogen or methane was 10%, the composition of the flue gas was similar to that of ammonia burning, as shown in Figure 13. When the methane co-firing rate was 30%, the concentrations of NOx and CO in the flue gas increased rapidly, and as the co-firing rate increased, hydrogen was found to be more advantageous in terms of environmental emissions.

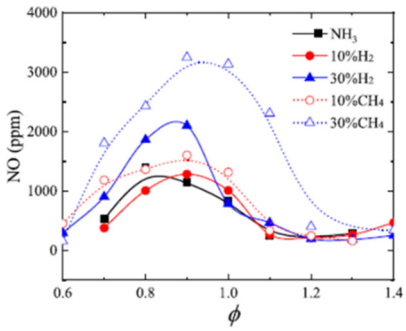

(**a**) NO with equivalence ratio

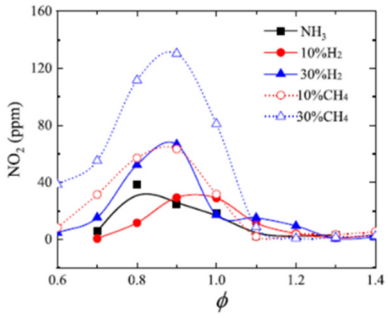

(**b**) NO_2 with equivalence ratio

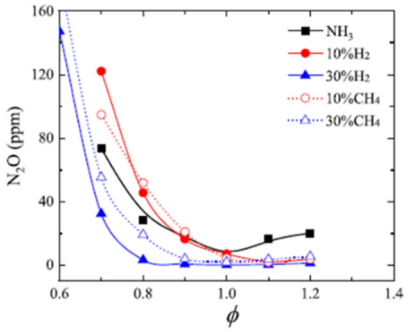

(**c**) N_2O with equivalence ratio

Figure 13. NOx emissions with equivalence ratio for H_2 and CH_4 blend fraction: (**a**) NO; (**b**) NO_2; (**c**) N_2O. Courtesy of Elsevier [69].

In other experimental research activities, results regarding flame characteristics for ammonia-methane co-firing [70–75], ammonia-hydrogen co-firing [76–79], and ammonia-syngas co-firing [80] have been reported, respectively. As a common opinion, it was reported that the ignition characteristics and flame velocity were improved when gas fuel with a higher reactivity than ammonia was mixed. Chai et al. reviewed the combustion characteristics of ammonia-mixed fuel gas [81].

2.5. Oxygen Enrichment and Plasma Application for Ammonia-Flame Enhancement

As mentioned earlier, there are several methods for flame stabilization. The method of injecting pure oxygen instead of air as an oxidizing agent or increasing oxygen concentration is a traditional scheme. In ammonia combustion, it has been attempted to improve the stability of ammonia flame through oxygen enrichment [82–89]. Figure 14 shows that turbulent flame speed increases with the intensity of turbulence and higher oxygen concentration [83]. This leads to higher flame temperatures and improves burning flame velocity. Figure 15 indicates that oxygen enrichment accelerates the spherically expanding flames and consequently reduces the buoyancy effect on the flame propagation [85].

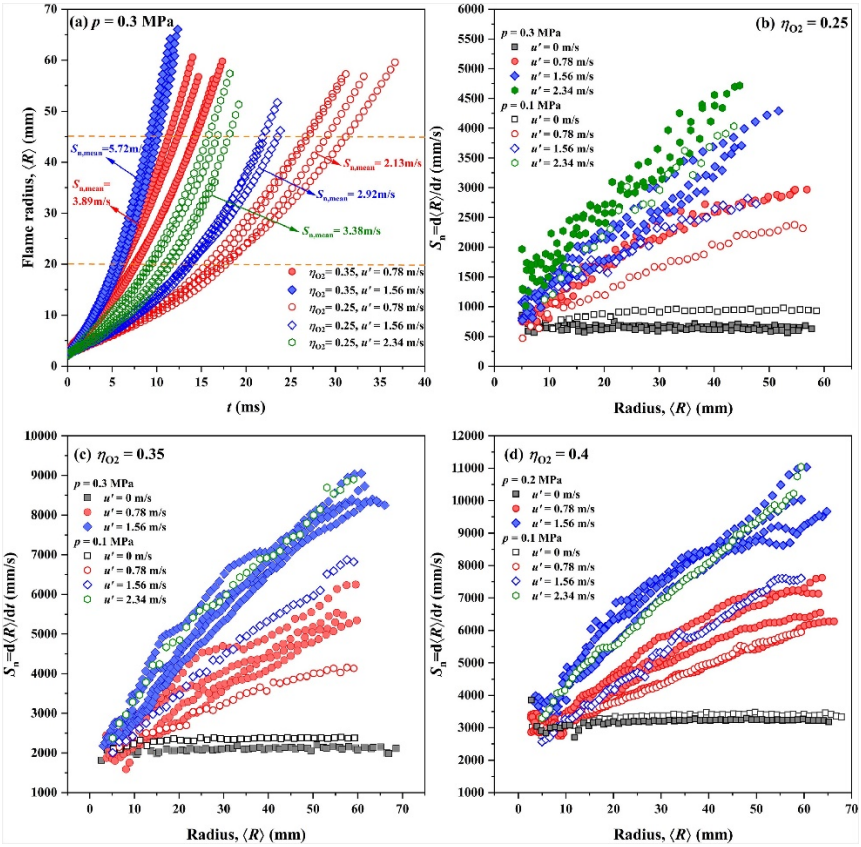

Figure 14. Flame radius verses time and turbulent flame speed against mean flame radius with increasing turbulent intensity, O_2 concentration and pressure at 298 K. Courtesy of Elsevier [83].

Recently, research on stabilization of ammonia flame through plasma has also been conducted [90]. This is a usual method for flame stabilization that has been performed for a long time [91–96]. However, in this study, it was experimentally demonstrated that flame stabilization and NOx generation could be simultaneously reduced through plasma-assisted combustion. The authors concluded that a large quantity of HO_2 is formed in the plasma region and the HO_2 consumes NO and NO_2 through chemical reactions NO + HO_2 → OH + NO_2 and NO_2 + HO_2 → HONO + O_2. For NH_2, NO + NH_2 → NNH + OH and NH_2 + NO → N_2 + H_2O are shown in Figure 16.

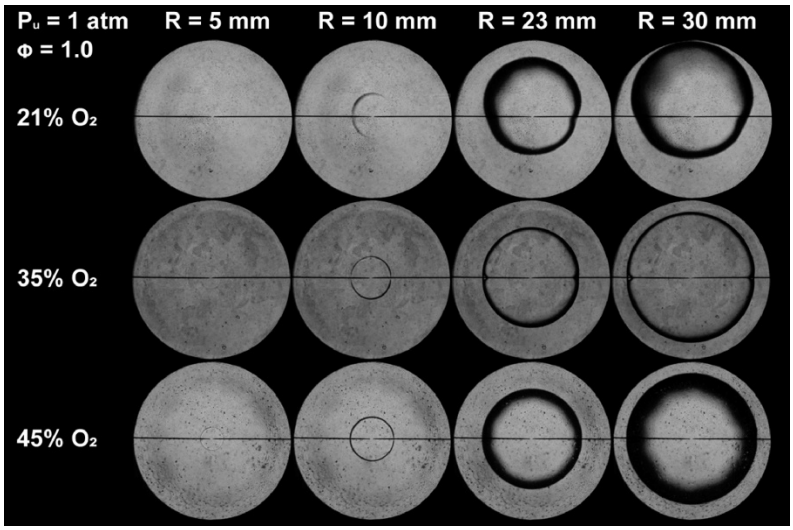

Figure 15. Schlieren images of stoichiometric NH_3-O_2-N_2 flames with the O_2 content varying from 21% to 45% at 1 atm. Courtesy of Elsevier [85].

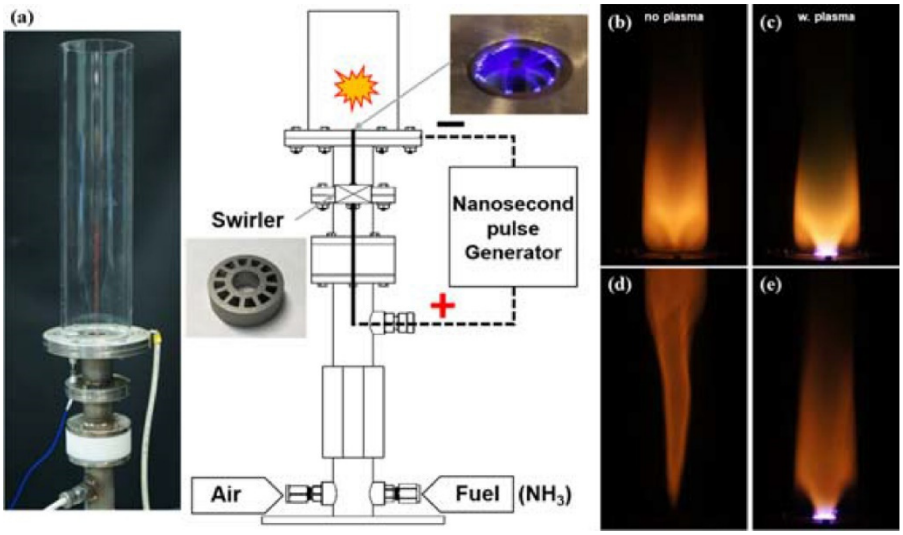

Figure 16. Experimental apparatus and direct photographs of flame with and without plasma: (**a**) Combustor; (**b**) and (**c**) are at φ = 0.94, (**d**) and (**e**) are at φ = 0.71. Courtesy of Elsevier [90].

3. R&D Activities on Gas Turbine System

3.1. Lab-Scale Model Burner for Ammonia-Rich Mixture Combustion

A research team from Cardiff University in the UK worked on an ammonia gas turbine [97–100]. The superiority of ammonia as a storage material for hydrogen and the possibility for direct combustion was evaluated. Finally, they announced that an ammonia-hydrogen dual-fuel approach will be applied in their facility, with the hydrogen generated in a pre-combustion ammonia cracking step. Valera-Media et al. conducted an experiment for stable combustion operation when hydrogen was added using a 70% NH_3-30% H_2 (mol%) blend [97].

Figure 17 shows an optical generic swirl-burner and OH* intensity results. Under fuel-rich conditions, the measurement results showed that the OH* intensities were still high, along with an increase in the consumption of OH* at the flame front at high inlet temperatures. They also investigated ammonia-methane combustion in swirl burners, as shown in Figure 18 [98]. A fully premixed injection was not appropriate for optimized ammonia combustion, and flame instabilities were produced at a medium swirl burner; hence, a lower swirl and another injection method were required.

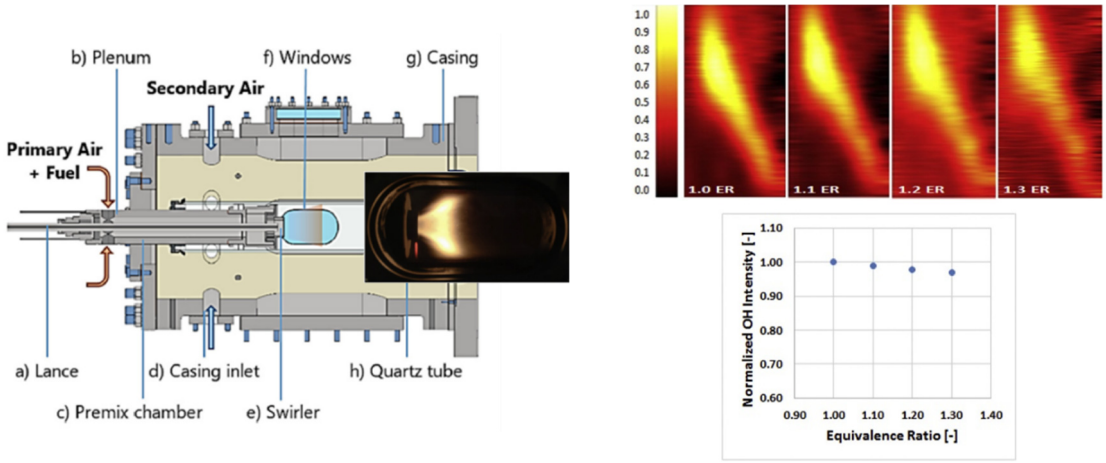

(**a**) Burner schematic (**b**) Gas turbine system for 50 kW

Figure 17. Burner device and visualization results to investigate H_2-NH_3 mixed combustion characteristics: (**a**) Burner schematic; (**b**) De-convoluted OH intensity at different φ and normalized intensities at highest value (φ = 1.0). Modified from [97]. Courtesy of Elsevier [97].

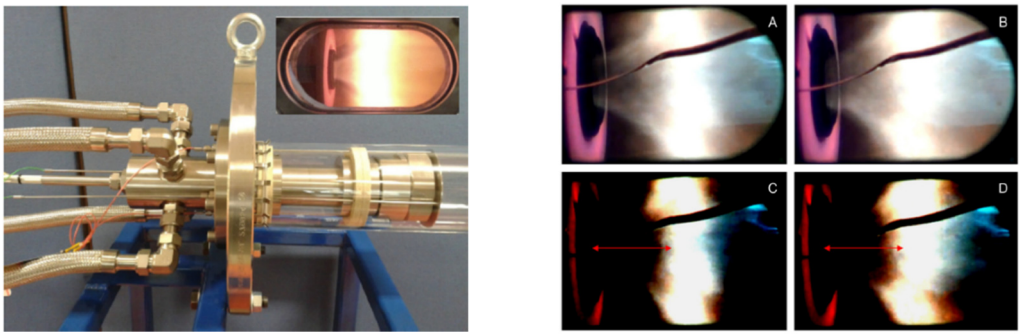

(**a**) Generic swirl burner (**b**) Instantaneous images on flame instability

Figure 18. Gas turbine model combustor and direct images on NH_3-CH_4 flames of 61% NH_3 and 39% CH_4: (**a**) Gas turbine model combustor with NH_3-CH_4 blend flame at equivalence ratio 1.31 for 31.7 kW; (**b**) Instantaneous photographs on flame position change (instability). Modified from [98]. Courtesy of Elsevier [98].

3.2. 50 kW Small-Scale System

A research team in Japan succeeded in generating a 41.8 kW class gas turbine using ammonia as fuel. This development was carried out in close cooperation with the group at Tohoku University and the National Institute of Advanced Industrial Science and Technology (AIST). The combustion and power generation system optimized for bi-fuel supply was developed by remodeling the combustor of Toyota Turbine and System Inc.'s micro gas turbine. In the early stage of development, approximately 30% of ammonia was mixed with methane to generate 21 kW of power. Subsequently, R&D was carried out with the goal of operating a gas turbine using ammonia as the main fuel. In 2016, the ammonia supply facility and the methane supply facility were repaired, and a demonstration test for gas turbine power generation using ammonia as the main fuel was conducted. The main performance goals were to maintain compatibility with the existing power generation system and to minimize NOx emissions.

Figure 19 shows the ammonia combustor (prototype bi-fuel combustor) and the overview of the gas turbine system. Although NOx concentration in the exhaust gas of ammonia combustion exceeded 600 ppm, as shown in Figure 20, NOx removal equipment (SCR) can reduce NOx concentration below 10 ppm [101]. They have reported the results

of related studies every year, and recently [102–106], they have also conducted research on burning liquid ammonia by directly spraying it into a combustor [107].

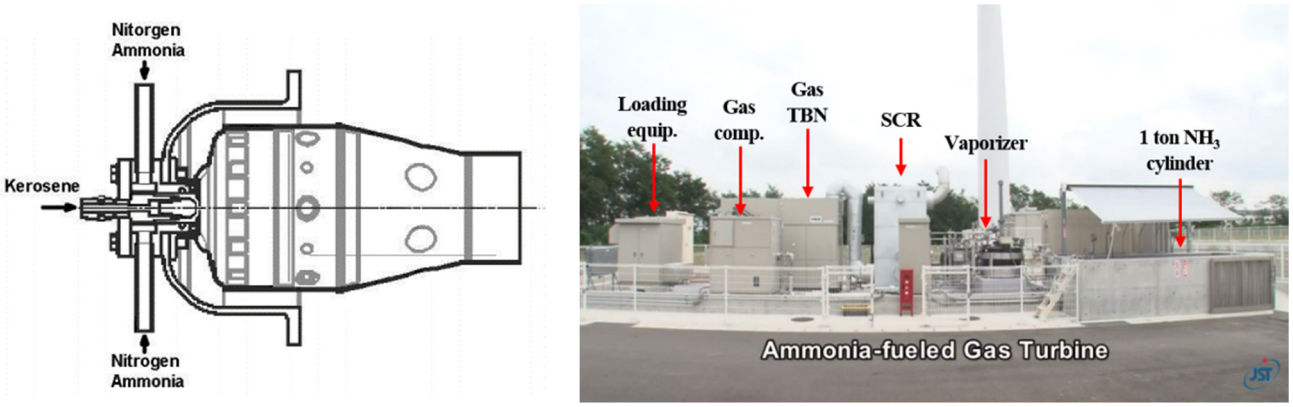

(**a**) Combustor shape (**b**) Gas turbine system for 50 kW power generation

Figure 19. 50 kW class NH_3 burning gas turbine combustor and power generation system: (**a**) NH_3 combustor for prototype bi-fuel combustion; (**b**) Test facilities for micro gas turbine power generation with large amount of NH_3 gas supply (1 ton cylinder). Modified from [101]. Courtesy of Ammonia Energy Association [101].

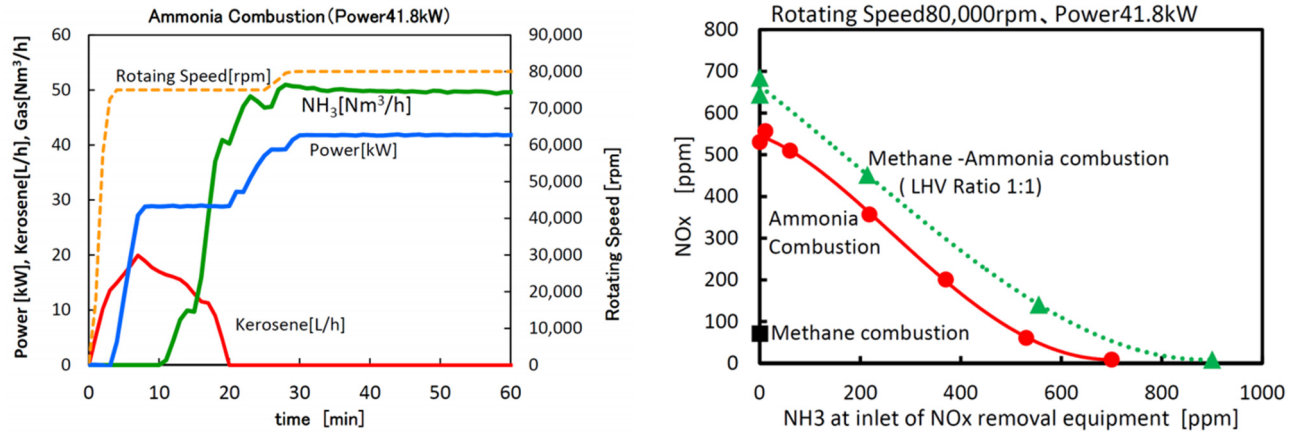

(**a**) Operation data on 100% NH_3 combustion (**b**) NOx emission

Figure 20. Operational power and NOx emissions of NH_3 combustion gas turbine: (**a**) Power output during NH_3 combustion; (**b**) NOx emissions at rotating speed 80,000 rpm and power 41.8 kW. Modified from [101]. Courtesy of Ammonia Energy Association [101].

3.3. 2 MW Medium-Scale System

IHI Corporation is a representative company participating in the organization for the commercialization of ammonia combustion technology for gas turbines, coal-fired power plants, and fuel cells in the SIP program. IHI evaluated the NOx emission characteristics and efficiency of the power generation system by co-firing ammonia up to 20% based on the calorific value in the existing 2 MW_e class LNG gas turbine [108,109]. Figure 21 shows the overview of the gas turbine of the power generation system. When ammonia was not added during rated load operation, about 100 ppm of NOx was emitted; however, as the co-firing rate of ammonia increased, the NOx emission increased up to three times. Similar to the results of AIST, in this study, NOx emissions of up to 6 ppm were achieved using the downstream SCR facility, and performance to satisfy environmental regulations was secured using a commercial SCR facility. A dramatic increase in NOx emissions during ammonia co-firing is an issue that must be overcome, and to apply ammonia to a medium-

to-large gas turbine system in the future, it is necessary to minimize NOx emissions from the combustor itself.

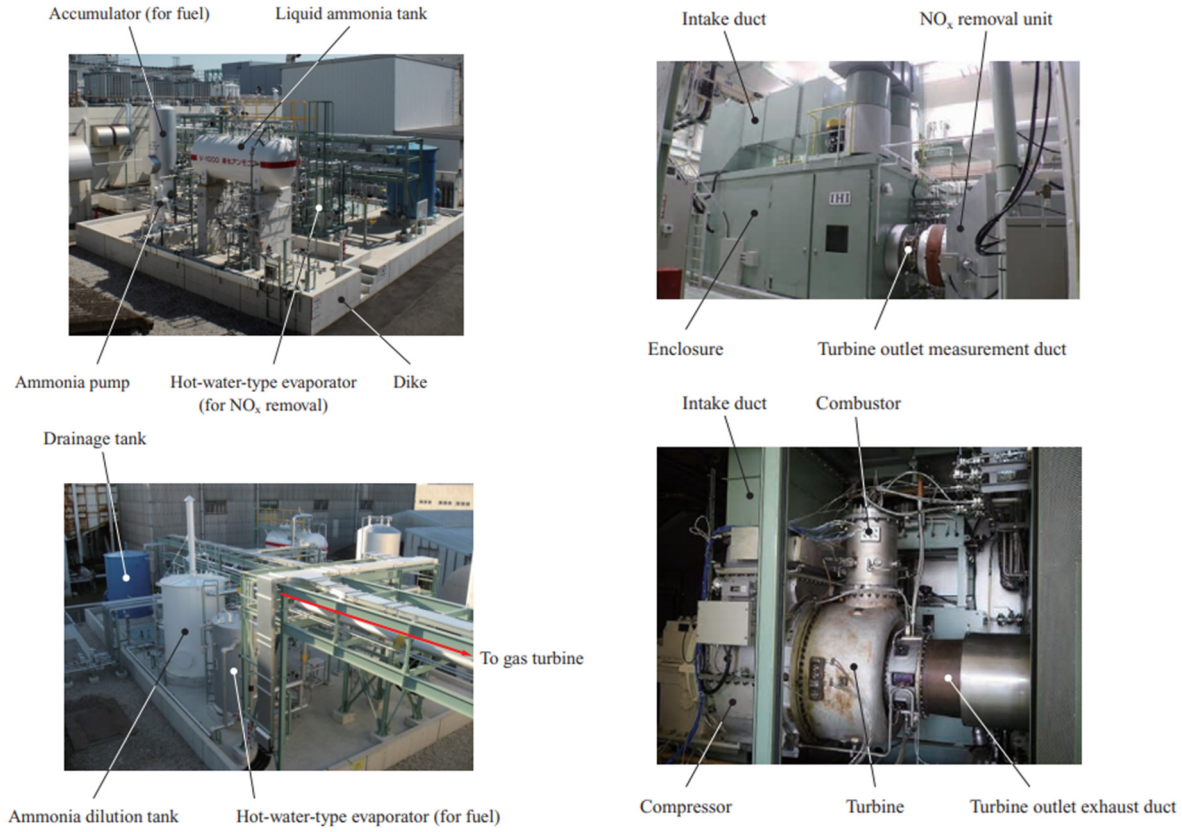

(**a**) Front overview (**b**) Gas turbine

Figure 21. IHI's 2 MW-class NH_3 gas turbine system: (**a**) Apparatus of NH_3 supply unit; (**b**) Apparatus of gas turbine. Modified from [109]. Courtesy of Ammonia Energy Association [109].

When the ammonia co-firing rate was 5%, the efficiency tended to decrease slightly; however, when the ammonia co-firing rate was 10% or more, the overall efficiency increased. As the mixing ratio was controlled based on the calorific value, the input amount of ammonia having a relatively low calorific was increased, and thus the turbine inlet flow rate increased, as shown in Figure 22.

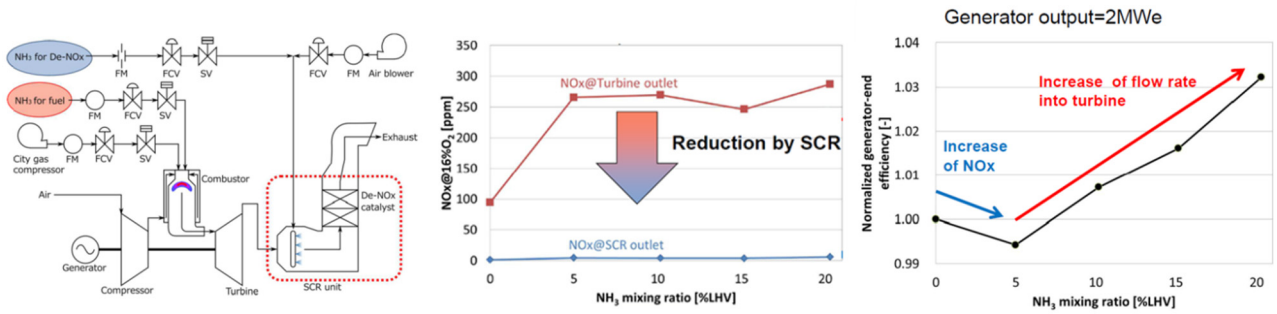

Figure 22. Schematic diagram of gas turbine system and experimental results: NOx emission and changes in power generation efficiency to the ratio of mixed NH_3. Modified from [109]. Courtesy of Ammonia Energy Association [109].

Recently, IHI announced that it has raised the liquid ammonia co-firing ratio on a 2 MW-class gas turbine to 70% on a heating value basis [110]. This technology enables the spraying of liquid ammonia directly into the combustor for mixing with natural gas while

constraining NOx emissions. IHI has attained 100% liquid ammonia-fueled combustion with this technology on a limited basis. It aims to ensure operational stability and suppress NOx and other emissions for commercializing a fully ammonia-fired gas turbine by 2025.

3.4. Developmet Plan of Commercial Large-Scale System

Hundreds of MW-class large gas turbines are being developed mainly for fuel supply systems. Unlike small- and medium-sized systems, large gas turbines are expected to have more severe restrictions on the size of the combustor for complete combustion of ammonia and more difficult control of NOx under high-temperature combustion conditions. Mitsubishi Power announced the start of the development of a 40 MW-class ammonia gas turbine in March 2021, and aims to commercialize it in 2025 after undergoing combustion and related operation tests [111]. Again, a technical bottleneck is the generation of NOx due to the nitrogen component of the fuel, and Mitsubishi is trying to solve the problem with a new ammonia combustor and SCR in the H-25 series gas turbine. Figure 23 shows the H-25 series gas turbine model of Mitsubishi.

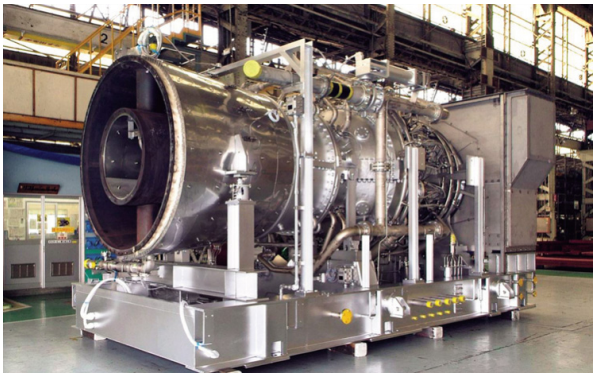

Figure 23. Mitsubishi H-25 series gas turbine [111].

General Electric (GE) and IHI have signed a memorandum of understanding for the development of a retrofit of an existing gas turbine for the combustion of ammonia fuel and a new gas turbine [112]. As the ammonia gas turbine market is widely distributed in Asia, including Korea and Japan, GE seems to have an idea to use ammonia in their own gas turbine technology. IHI is also planning to strengthen IHI's competitiveness through GE, which has flexible fuel combustion technology in the gas turbines.

4. R&D Activities on Coal-fired Power System

4.1. Fundamental Coal-Ammonia Combustion Characteristics

Studies on the fundamental characteristics of coal-ammonia mixed combustion technology were recently presented at the 38th International Combustion Society. Xia et al. conducted an experiment to examine the characteristics of spherical flame propagation in a turbulent flow field during the co-firing of pulverized coal and ammonia fuel [113,114]. The spherical propagation velocity of the coal-ammonia flame was faster than that of coal burning under all conditions, regardless of the ammonia-oxidizer equivalent ratio; however, the velocity changed according to the ammonia-oxidizer equivalent ratio. In the lean condition of ammonia fuel, a luminous flame by combustion of coal particles was emitted as radiant heat, and at the same time, the local equivalence ratio was increased in the flame zone due to the addition of volatile matter emitted from the coal particles, thereby increasing the flame propagation velocity. Moreover, as there is enough oxygen to react with the volatile matter, the authors created a scenario in which this leads to an increase in the propagation velocity. Conversely, in the rich condition of ammonia fuel, a luminous flame was not formed, and a large amount of thermal energy was used to increase the temperature of the particles. As a result, the volatile matter emission rate was slowed. In addition, the amount of local oxygen used for combustion was small, resulting

in a relatively slow flame velocity. Figure 24 shows the experimental apparatus and the image processing procedure to derive the propagation velocity of spherical flame.

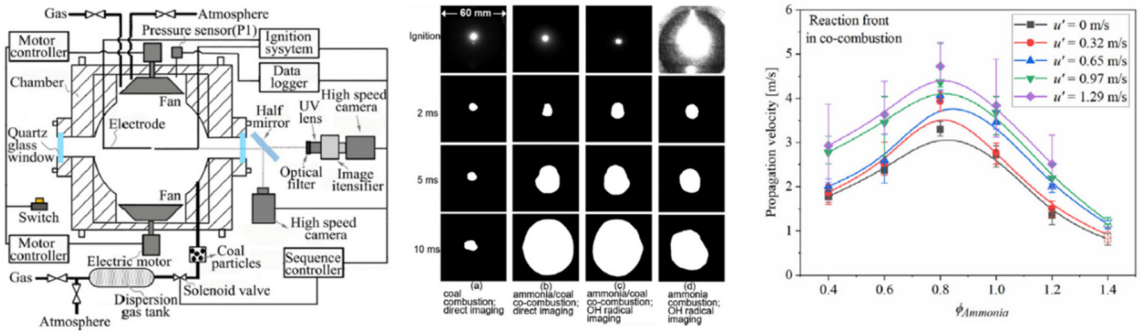

Figure 24. Experimental apparatus and results for obtaining the spherical propagation velocity of coal-NH_3. Reaction front propagation velocities as φ_{NH3} under various turbulence intensity, u'. Courtesy of Elsevier [113,114].

4.2. MW Medium-Scale System Experiment

The Central Research Institute of Electric Power Industry (CRIEPI), one of Japan's coal combustion research institutes, has conducted a co-firing experiment in a single burner test furnace for the generation of fuel-NOx, a key problem to overcome while using ammonia as a fuel. Figure 25 shows the facilities of the burner and the test furnace, and the experimental conditions. The combustion load was 760 kW (=100 kg/h), the oxygen concentration at the rear of the combustion chamber was 4%, and the air volume for multi-stage combustion was 30% of the total air volume [115]. The injection location was set as a variable with a maximum co-firing rate of 20%. When ammonia is injected into the pulverized coal burner and combusted, and the co-firing rate is less than 10%, it is at a level similar to the amount of NOx generated during conventional coal combustion. The NOx concentration increased with the increase of the co-firing rate. As a result, it was possible to reduce NOx generation by injecting ammonia at an optimal distance from the burner. This is because the selective non-catalytic reduction (SNCR) reaction reduces the amount of NOx generated. In addition, when ammonia was injected into the coal burner, the flame temperature was lowered, resulting in more unburned coal. However, the amount of unburned ammonia was extremely small, even during co-firing.

The goal of IHI was to demonstrate an existing 1000 MW-class coal-fired power plant after a co-firing test in a 10 MW_{th} test boiler, as shown in Figure 26 [116]. Based on the ammonia co-firing rate of 20%, the goal was to generate less than 200 ppm of NOx, and for this, the test was conducted with an input amount of 1.0–1.6 kg/h of coal and 0.4 ton/h of ammonia. As a result of the experiment, a stable flame was obtained through the swirl control of the combustion air, and the NOx concentration at 20% co-firing was measured to be equal to or lower than the value generated during 100% coal combustion. Ammonia and N_2O in the exhaust gas were below detectable levels. However, the particle emissivity and radiant heat transfer were reduced due to the decrease in coal usage, so the heat flux to the boiler wall was reduced. It was estimated that this was due to the change in the properties related to heat transfer [117]. In addition, the amount of NOx generated varied depending on the location of ammonia injection, and in the case of optimization, the NO concentration was measured to be lower than that during coal burning. This was because ammonia contributed to the denitrification reaction during ammonia injection. When ammonia was injected into the flame area at a distance from the burner tip, it led to a greater reduction of NOx and CO in quantity than when ammonia was injected from an inlet with coal particles based on 20% ammonia co-firing condition.

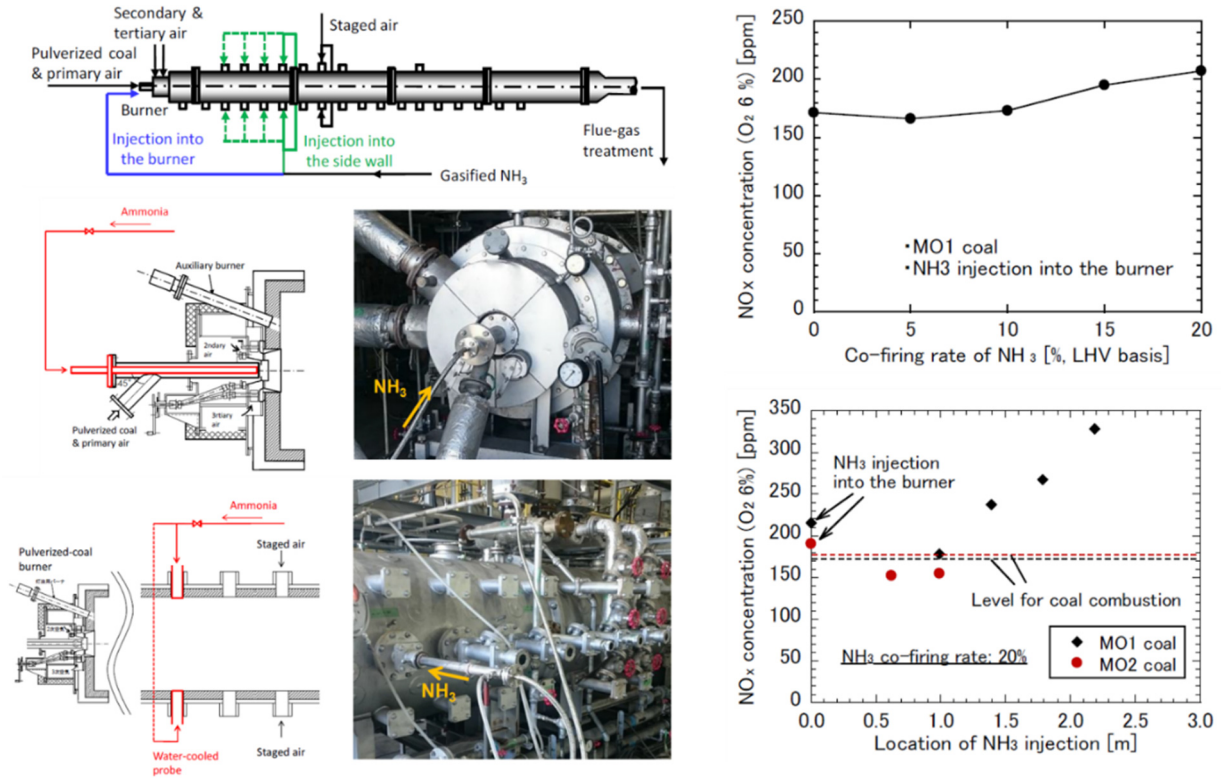

(**a**) Experimental facility (**b**) NOx concentration

Figure 25. Horizontal pulverized coal furnace in CRIEPI: (**a**) Schematic of combustion system; (**b**) NOx concentration measured. Modified from [115]. Courtesy of Ammonia Energy Association [115].

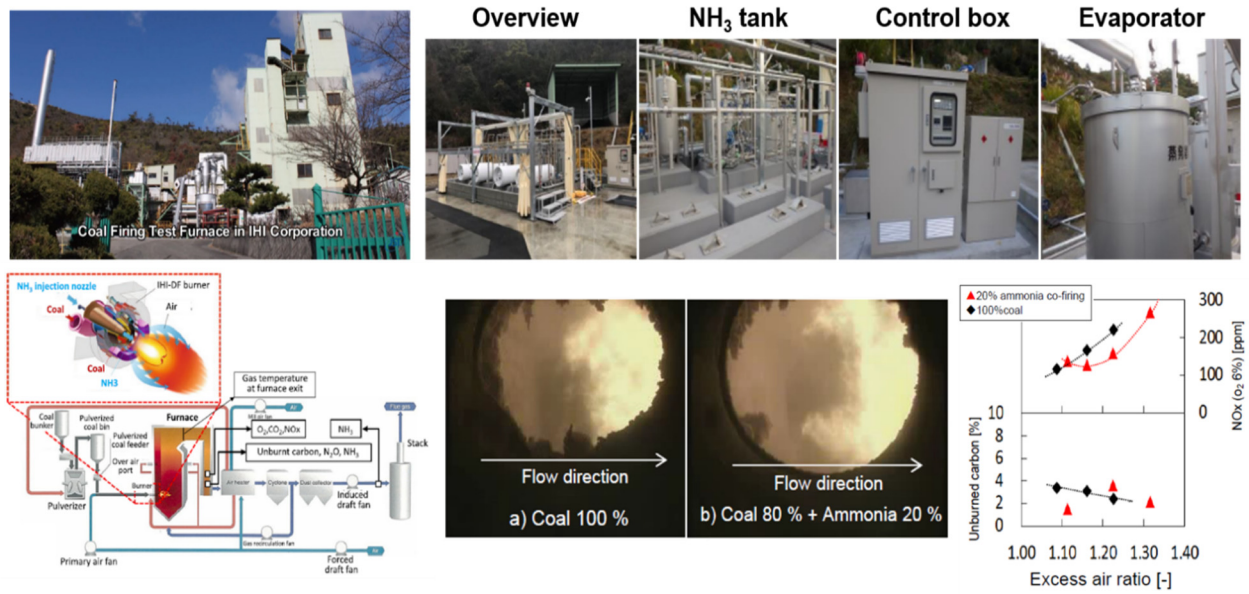

Figure 26. Coal firing test furnace and NH_3 feeding facilities in IHI. Modified from [116]. Courtesy of Ammonia Energy Association [116].

4.3. Commercial Large-Scale System Demonstration

Chugoku Electric Power attempted a coal-ammonia co-fired power plant in Japan's Mizushima power plant unit 2 (156 MW output). In this demonstration test, the CO_2 emissions were reduced by the amount of ammonia co-fired, and there was no change in the metal temperature of the heat exchanger, such as in the superheater and reheater. The

ammonia used as fuel was completely burned and not discharged to the outside. It was confirmed that the environmental standards were satisfied without any difference. The co-firing rate was 0.6% to 0.8% due to the capacity restrictions of the ammonia vaporizer; however, above all, it was confirmed that the coal-ammonia co-firing technology can be applied without any problem to power plants in commercial operation as a measure to reduce greenhouse gas emissions. Figure 27 shows an overall overview of the project [118].

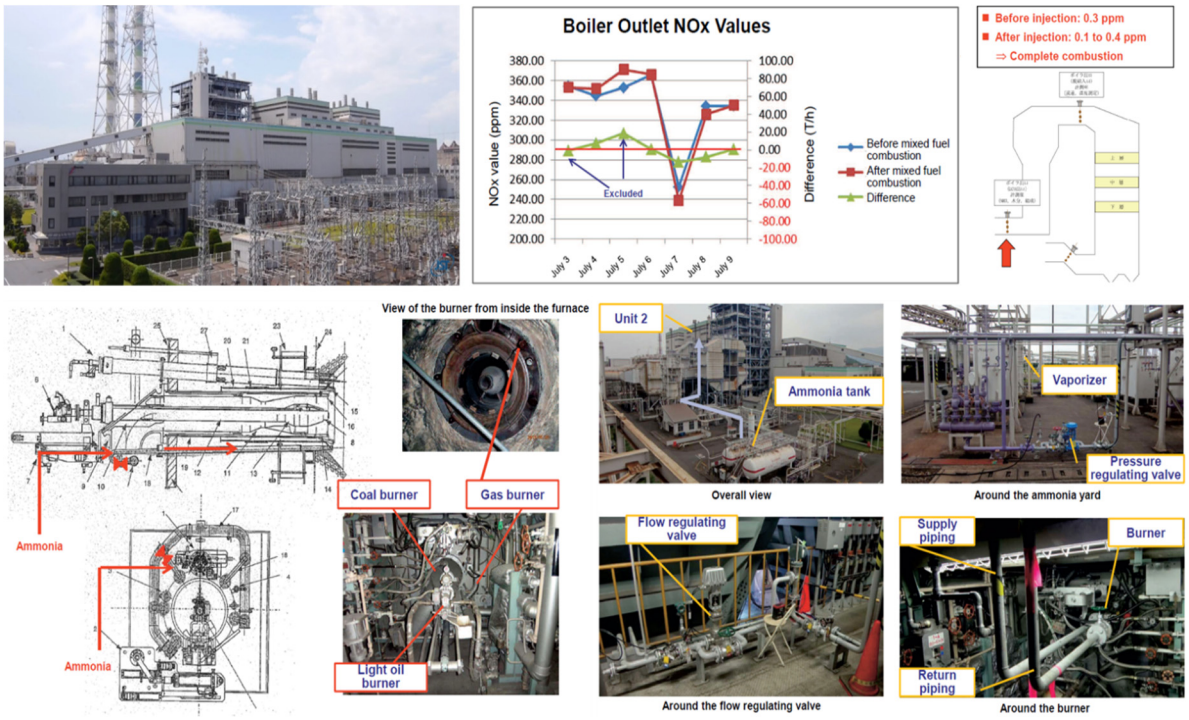

Figure 27. Burner structure and demonstration facilities in Mizushima power station unit 2. Modified from [118]. Courtesy of the Combustion Society of Japan [118].

A Japanese power generation company, JERA, plans to close all inefficient coal-fired power plants by 2030 and introduce ammonia combustion technology to coal-fired power plants by 2040. JERA and IHI announced that they would demonstrate 20% ammonia co-firing technology in a 1000 MW-class coal-fired power plant. The period of the research and demonstration project is from June 2021 to March 2025. The target power plant is Hekinan power plant unit 4, and the goal of the demonstration project is to prove and build co-firing technology in a large-capacity commercial plant, check boiler heat absorption, and evaluate the environmental impact of exhaust gas. It is planned to partially modify the design of the 48 burners for optimal injection of ammonia. IHI will be in charge of the burner development, and JERA will be in charge of ammonia procurement and related construction. Figure 28 shows a conceptual diagram of the ammonia combustion plan in the target power plant and boiler [119].

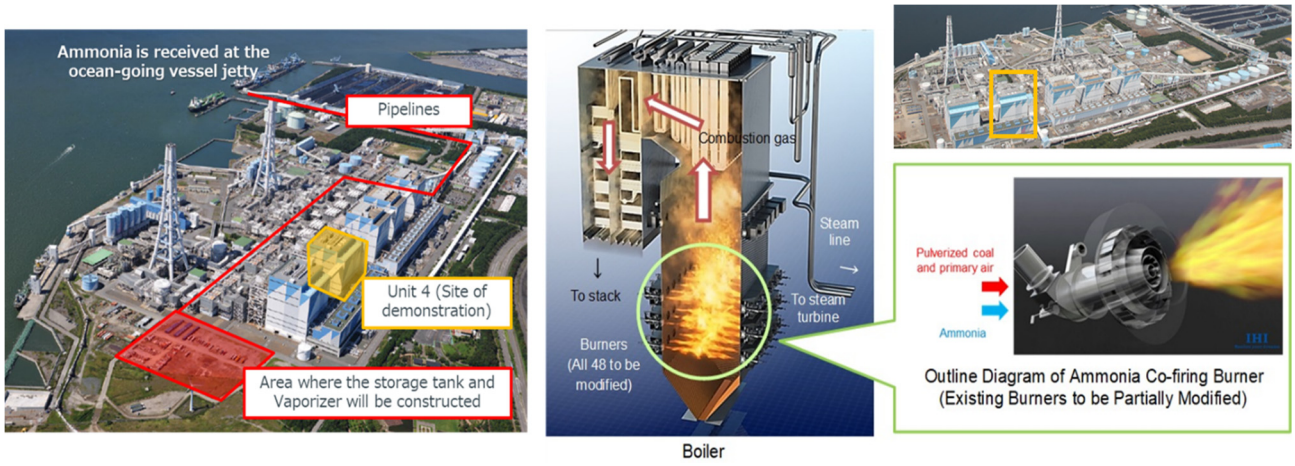

Figure 28. Boiler retrofit concept and overview of Hekinan power station unit 4. Modified from [119].

5. Ammonia Combustion Experiments in Korea Institute of Energy Research

In this section, we briefly report the information regarding an ammonia combustion experiment conducted by Korea Institute of Energy Research. A preliminary experiment was conducted to observe the characteristics of ammonia burning flame for gas turbines and coal co-fired flame for coal fired boiler applications. This experiment was conducted in accordance with the safety regulations put forth by the Korean government on the use of toxic gases.

5.1. Experimental Appratus and Method

Figure 29 shows the schematics of the model combustor and the experimental apparatus. The combustor was swirl stabilized with a bluff body. The axial swirler fitted to a central support rod has eight vanes with a swirl angle, $\alpha = 45°$. According to the formula, swirl number was estimated to be 0.77 [120]. High purity NH_3 (99.99%) and dry air, accurately metered by mass flow controllers (Brooks 5850E) within 2% error, were fully premixed before being supplied to the combustor. The detailed device structure was presented in the following paper [121]. The ammonia flow rate was 22 SLPM (5 kW_{th} capacity), and the air flow rate was determined based on the equivalence ratio of 1. When coal-ammonia-air combustion experiment was conducted, the ammonia flow rate was reduced to fix the total capacity to 5 kW_{th}. In the lower part of the combustor injector, a honeycomb (20 mm in length) was installed to straighten the mixture flow uniformity. An inverted cone-shape bluff body, whose flat surface was extruded from the dump plane, was used to enhance the flame stabilization. A quartz tube was built for liner role and flame visualization. The flame was observed using a Sony FDR-AX700 camera.

The proximate and ultimate analysis data of the fuel coal are presented in Table 2. The particles within a size range of 100~125 μm were dropped down slowly into a glass funnel by a micro-syringe injector and were entrained with a carrier gas at room temperature, as described in Figure 29. The flow rate of the carrier gas was independently controlled considering the mass of solid particles falling into the glass funnel. This design allowed the number and density of particles and main air flow rate to be varied independently. When the coal-ammonia-air combustion experiment was conducted, particle feeding rate was kept to 0.02–0.1 g/s to observe the behavior according to co-firing rate 10–50%. The gas condition was not affected by particle combustion. The equipment for the supply system, including the coal feeder, is detailed in a study carried out by Lee and Choi [122–124].

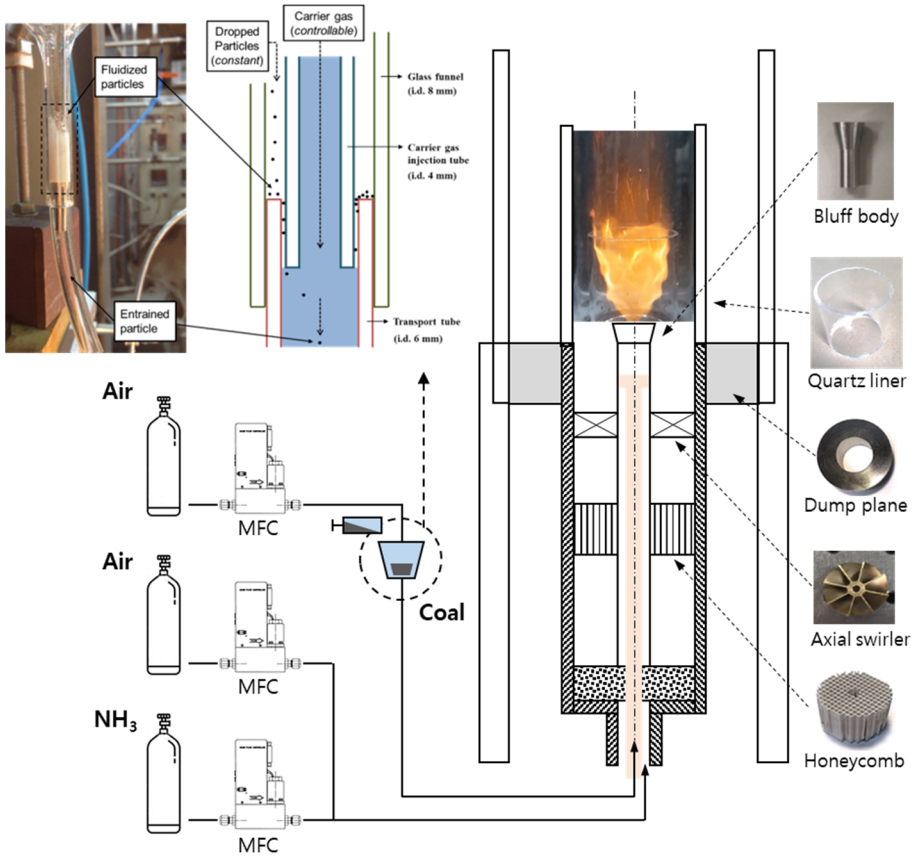

Figure 29. Experimental apparatus for NH_3-air and NH_3-coal-air combustion.

Table 2. Coal properties.

Rank	Proximate (Air-Dried) (wt%)				Ultimate (Air-Dried) (wt%)					Heating Value (MJ/kg)
	W	V.M.	F.C.	Ash	C	H	O	N	S	
Bituminous	2.38	35.32	49.62	12.68	70.38	4.65	7.91	1.48	0.52	27.98

5.2. Flame Observation on Gaseous Ammonia and Co-Fired with Coal Particles

Figure 30 shows an ammonia burning flame and an ammonia-coal co-fired flame. Because of the slow reaction rate of ammonia and the narrow flammability limit, it was judged that a premixed flame was more appropriate than a diffusion flame. In this experiment, a premixed flame was formed and observed. Ignition of gaseous ammonia fuel in the cold state was not easy, but ignition was easily achieved when the combustor was sufficiently warmed up. However, after being ignited once, the flame was maintained at an equivalence ratio of 1.0, or in a somewhat fuel-rich state. This phenomenon occurred due to the narrow flammability limit and high ignition energy, which can be explained by the results of related previous studies, as mentioned in Section 2. When the ammonia flame was extinguished, there was a peculiar smell of ammonia; however, when the flame was attached, the smell was not felt.

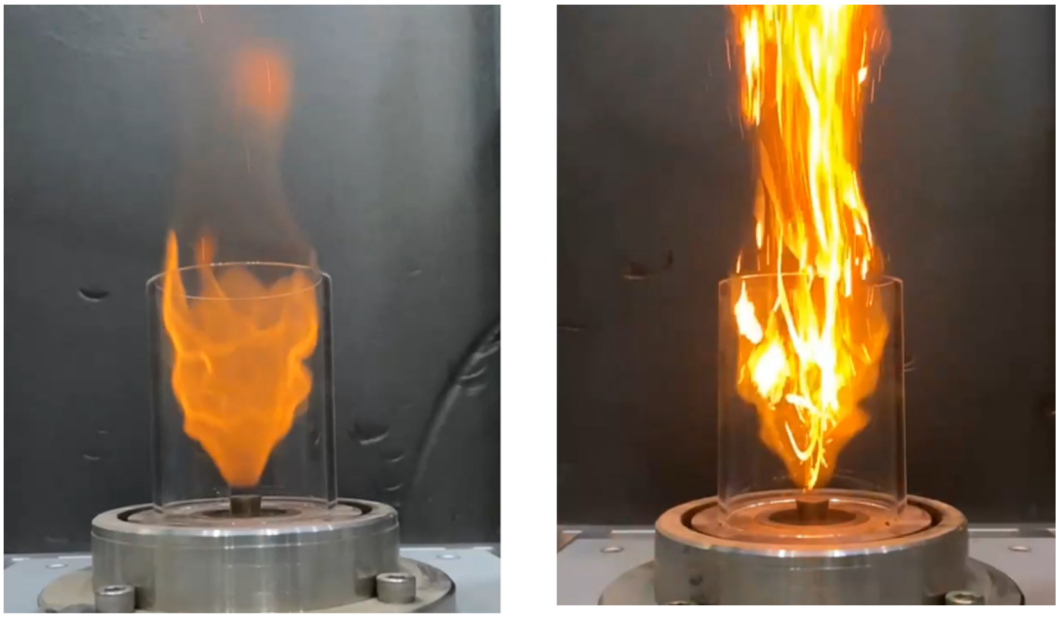

(**a**) Ammonia-air combustion (**b**) Ammonia-coal-air combustion

Figure 30. Flame observation results at 5 kW_{th} capacity: (**a**) Flame visualization for 100% NH_3 combustion; (**b**) Flame visualization for 30% NH_3 and 70% coal combustion.

Coal particles burned relatively well with ammonia flame, which has a relatively low flame temperature. The ammonia-coal flame showed a longer shape than when gaseous ammonia was burned alone, as shown in Figure 30. Consequently, it is considered to be the result of taking longer time for volatile matter and char combustion processes. There will be effects depending on the particle size and the type of coal; however, as the current study was conducted with only one type of coal and particle size, we plan to proceed with this work in future research. Ammonia-coal flames in burner types, not spherical flames, are reported for the *first time* in this study. As the experimental device is designed as a model of a gas turbine combustor, we plan to re-create an experimental facility suitable for coal-fired burners.

6. Conclusions

Ammonia, a carbon-free fuel, is being studied mainly in many countries to reduce CO_2 emissions. In particular, Korea and Japan, as countries with some of the top 10 greenhouse gas emissions in the world, are making great efforts to reduce carbon emissions. Technology development for the use of carbon-free fuels such as hydrogen and ammonia is intensively in progress, and research for ammonia direct-combustion and hydrogen production by the cracking of ammonia as an enabler towards a hydrogen society are in progress. Ammonia is a part of hydrogen fuel as an energy carrier rather than a separate fuel, and the use of ammonia will drive development towards a hydrogen society faster.

Thermal power plants, including coal-fired power plants and gas turbines, are a large source of CO_2 emissions, and the carbon emission reduction effect can be maximized when ammonia combustion is applied in the systems. However, there are still challenges to be solved for ammonia combustion technology to be commercialized in thermal power plants. As ammonia combustion features high NOx emissions and low flame stability, a meticulous study is required. In fundamental experiment fields, burning velocity and ignition characteristics have been investigated in laminar and turbulent flow conditions. In addition, flame structures and associated reaction mechanisms have been numerically investigated under pressure conditions up to 5 bar for application to gas turbines. These fundamental results can provide insight for future scale-up and engineering for commercialization. In the gas turbines, the combustor pressure is 20 bar or more, and experimental results in such

a high-pressure environment are necessary. In high-pressure conditions, the NOx formation mechanism should be investigated based on the experimental results, at the same time. Ammonia combustion or co-firing mechanisms should be elucidated in terms of chemical kinetics in detail. This information is important to prevent excessive NOx generation and enhance flame stabilization. Likewise for coal-ammonia co-combustion, an accurate reaction mechanism must be derived beyond the current level of reaction scenario prediction in order to present a solution based on physical theory rather than research based on experience. It enables design optimization of burners. In fundamental research, the weak flammability of ammonia-air flame could be enhanced through substituting other fuels such as methane and hydrogen for ammonia, preheating inlet gases, and increasing oxygen concentration. However, it is difficult to inject additional fuel gases or pure oxygen into a practical combustion system for power generation. The fuel co-firing in ammonia requires additional expenses because it is accompanied by a gas supply facility, pipeline, control, and safety system. It is necessary to develop a combustion technology that can reduce NOx emissions without downstream equipment such as SCR for gas turbine applications. The current NOx emission level during ammonia combustion in gas turbine experiments is several hundred ppm, and NOx emission produced from combustion has been separated through the downstream facility. Strictly speaking, this approach offsets the benefits of using carbon-free ammonia fuels. Therefore, it is necessary to develop a technology to reduce NOx generation, for example, by deriving SNCR reaction during combustion. In the most common way, the methods such as multi-stage (rich-lean) combustion have been used to reduce NOx practically.

At the pilot or demonstration experimental level, design technology should be verified. Most plant operators are retrofitting the existing facilities to reduce costs. As a power plant is a large-scale facility, the investment amount is large and the risk is large in hardware replacement. Therefore, it is important to obtain accurate data while changing many factors during pilot- and demo-scale experiments. Among the results currently reported, in the case of coal-fired power plants, the ammonia co-firing rate in large power plants is less than 1%. Although it was reported that there were no differences from the previous operation results, problems that may occur when the ammonia co-firing rate increases by 20% or more are expected. As the flame temperature decreases, for example, the amount of heat transfer to the water-steam pipe will decrease, which will change the steam output of the boiler. Along with this, there is a possibility of unburned carbon generation, and it may be necessary to control the amount of oxidizing agent for complete combustion in over-fire air ports. Therefore, to apply the ammonia co-firing technology in the existing boiler, the boiler water circulation system analysis should be accompanied and reviewed with corrosion between unburned ammonia and metallic part. In ammonia co-firing demonstration studies, although it was announced that injecting ammonia together with coal particles at the center of the burner had a low NOx reduction effect, ammonia was injected into an oil burner for startup due to the difficulty of design changes. There are various injection methods such as spraying into the coal flame, for example, on a demo-scale to maximize ammonia utilization.

Many researchers are working to solve these issues, and the authors' institutions are also conducting research for this purpose. The present study reported the apparent observation of the pulverized coal-ammonia co-firing flame structure for the *first time*, and detailed analysis results will be continuously reported in the future. Ammonia combustion technology, centered on gas turbines and coal-fired power plants, is in the full-scale demonstration stage, and the results will be reported from 2025 to 2030 in most projects. For carbon neutrality, combustion majors should strive with great responsibility in preparing for developing technology to reduce CO_2 emission. It is hoped that this study will be used as an informative resource for researchers working on carbon-free and high-efficiency ammonia combustion.

Author Contributions: Conceptualization, H.L.; Methodology, H.L.; Investigation, H.L. and M.-J.L.; Resources, H.L. and M.-J.L.; Data Curation, H.L. and M.-J.L.; Writing—original draft preparation,

H.L.; writing—review and editing, H.L. and M.-J.L.; visualization, H.L. and M.-J.L.; supervision, M.-J.L.; project administration, M.-J.L.; funding acquisition, M.-J.L. Both authors have read and agreed to the published version of the manuscript.

Funding: This work was conducted under the framework of the research and development program of the Korea Institute of Energy Research (C1-2460).

Institutional Review Board Statement: Not applicable.

Informed Consent Statement: Not applicable.

Data Availability Statement: Not applicable.

Conflicts of Interest: The authors declare no conflict of interest.

References

1. Biennial Update Report submissions from Non-Annex I Parties. Available online: https://unfccc.int/BURs (accessed on 30 July 2021).
2. Olivier, J.; Peters, J. *Trends in Global CO_2 and Total Greenhouse Gas Emissions: 2020 Report*; PBL Netherlands Environmental Assessment Agency: The Hague, The Netherlands, 2020.
3. Global Energy Review 2021 CO_2 Emissions. Available online: https://www.iea.org/reports/global-energy-review-2021/co2-emissions (accessed on 9 July 2021).
4. SIP-Energy Carriers. Available online: https://www.jst.go.jp/sip/k04.html (accessed on 5 August 2021).
5. Feasibility Study under NEDO Program on Ammonia Co-Firing in Thermal Power Generation Facility. Available online: https://www.jera.co.jp/english/information/20200327_479 (accessed on 5 August 2021).
6. Sanchez, A.; Castellano, E.; Martin, M.; Vega, P. Evaluating ammonia as green fuel for power generation: A thermos-chemical perspective. *Appl. Energy* **2021**, *293*, 116956. [CrossRef]
7. Yapicioglu, A.; Dincer, I. A review on clean ammonia as a potential fuel for power generators. *Renew. Sustain. Energy Rev.* **2019**, *103*, 96–108. [CrossRef]
8. Dreizler, A.; Pitsch, H.; Scherer, V.; Schulz, C.; Janicka, J. The role of combustion science and technology in low and zero impact energy transformation processes. *Appl. Energy Combust. Sci.* **2021**, *7*, 100040.
9. Zamfirescu, C.; Dincer, I. Using ammonia as a sustainable fuel. *J. Power Sources* **2008**, *185*, 459–465. [CrossRef]
10. Verkamp, F.; Hardin, M.; Williams, J. Ammonia combustion properties and performance in gas-turbine burners. *Proc. Combust. Inst.* **1967**, *11*, 985–992. [CrossRef]
11. Chiong, M.; Chong, C.; Ng, J.; Mashruk, S.; Chong, W.; Samiran, N.; Mong, G.; Valera-Medina, A. Advancements of combustion technologies in the ammonia-fuelled engines. *Energy Convers. Manag.* **2021**, *244*, 114460. [CrossRef]
12. Dimitriou, P.; Javaid, R. A review of ammonia as a compression ignition engine fuel. *Int. J. Hydrogen Energy* **2020**, *45*, 7098–7118. [CrossRef]
13. Martins, J.; Brito, F. Alternative fuels for internal combustion engines. *Energies* **2020**, *13*, 4086. [CrossRef]
14. Cardoso, J.; Silva, V.; Rocha, R.; Hall, M.; Costa, M.; Eusebio, D. Ammonia as an energy vector: Current and future prospects for low-carbon fuel applications in internal combustion engines. *J. Clean. Prod.* **2021**, *296*, 126562. [CrossRef]
15. Zamfirescu, C.; Dincer, I. Ammonia as a green fuel and hydrogen source for vehicular applications. *Fuel Process. Technol.* **2009**, *90*, 729–737. [CrossRef]
16. Miura, D.; Tezuka, T. A comparative study of ammonia energy systems as a future energy carrier, with particular reference to vehicle use in Japan. *Energy* **2014**, *68*, 428–436. [CrossRef]
17. Kroch, E. Ammonia–A fuel for motor buses. *J. Inst. Pet.* **1945**, 213–223.
18. Kong, S.; Reiter, A. Combustion and emissions characteristics of compression-ignition engine using dual ammonia-diesel fuel. *Fuel* **2011**, *90*, 87–97.
19. Kong, S.; Gross, C. Performance characteristics of a compression-ignition engine using direct-injection ammonia-DME mixtures. *Fuel* **2013**, *103*, 1069–1079.
20. Lhuillier, C.; Brequigny, P.; Contino, F.; Mounaim-Rousselle, C. Experimental investigation on ammonia combustion behavior in a spark-ignition engine by means of laminar and turbulent expanding flames. *Proc. Combust. Inst.* **2021**, *38*, 5859–5868. [CrossRef]
21. Oh, S.; Park, C.; Kim, S.; Kim, Y.; Choi, Y.; Kim, C. Natural gas-ammonia dual-fuel combustion in spark-ignited engine with various air-fuel ratios and split ratios of ammonia under part load condition. *Fuel* **2021**, *290*, 120095. [CrossRef]
22. Issayev, G.; Giri, B.; Elbaz, A.; Shrestha, K.; Mauss, F.; Roberts, W.; Farooq, A. Combustion behavior of ammonia blended with diethyl ether. *Proc. Combust. Inst.* **2021**, *38*, 499–506. [CrossRef]
23. Boretti, A. Novel dual fuel diesel-ammonia combustion system in advanced TDI engines. *Int. J. Hydrogen Energy* **2017**, *42*, 7071–7076. [CrossRef]
24. Grannell, S. The Operating Features of a Stoichiometric, Ammonia and Gasoline Dual Fueled Spark Ignition engine. Ph.D. Thesis, University of Michigan, Ann Arbor, MI, USA, 2008.

25. Jang, J.; Woo, Y.; Yoon, H.; Kim, J.; Lee, Y.; Kim, J. Combustion characteristics of ammonia-gasoline dual-fuel system in one liter engine. *J. Korean Inst. Gas* **2015**, *19*, 1–7. [CrossRef]
26. Al-Aboosi, F.; El-Halwagi, M.; Moore, M.; Nielsen, R. Renewable ammonia as an alternative fuel for the shipping industry. *Curr. Opin. Chem. Eng.* **2021**, *31*, 100670. [CrossRef]
27. Mckinlay, C.; Turnock, S.; Hudson, D. Route to zero emission shipping: Hydrogen, ammonia or methanol? *Int. J. Hydrogen Energy* **2021**, *46*, 28282–28297. [CrossRef]
28. MAN Energy Solutions is Developing a Fuel-Flexible, Two-Stroke Ammonia Engine as a Key Technology in the Maritime Energy Transition. Available online: https://www.man-es.com/discover/two-stroke-ammonia-engine (accessed on 12 August 2021).
29. World's First Full Scale Ammonia Engine Test—An Important Step towards Carbon Free Shipping. Available online: https://www.wartsila.com/media/news/30-06-2020-world-s-first-full-scale-ammonia-engine-test---an-important-step-towards-carbon-free-shipping-2737809 (accessed on 12 August 2021).
30. Daewoo Wins Approval for Ammonia-Fired Ship from Lloyd's Register. Available online: http://www.koreaherald.com/view.php?ud=20201006000301 (accessed on 12 August 2021).
31. Samsung Heavy Gets Nod for Ammonia-Fueled Ships from Lloyd's Register. Available online: https://en.yna.co.kr/view/AEN20200924003200320 (accessed on 12 August 2021).
32. Hyundai Mipo Gets Approval for Ammonia-Fueled Ships from Lloyd's Register. Available online: https://en.yna.co.kr/view/AEN20200723004600320 (accessed on 12 August 2021).
33. Boretti, A. Novel heavy duty engine concept for operation duel fuel H_2-NH_3. *Int. J. Hydrogen Energy* **2012**, *37*, 7869–7876. [CrossRef]
34. Wang, Y.; Zhou, X.; Liu, L. Theoretical investigation of the combustion performance of ammonia/hydrogen mixtures on a marine diesel engine. *Int. J. Hydrogen Energy* **2021**, *46*, 14805–14812. [CrossRef]
35. Morch, C.; Bjerre, A.; Gottrup, M.; Sorenson, S.; Schramm, J. Ammonia/hydrogen mixtures in an SI-engine: Engine performance and analysis of a proposed fuel system. *Fuel* **2011**, *90*, 854–864. [CrossRef]
36. Kim, K.; Roh, G.; Kim, W.; Chun, K. A preliminary study on an alternative ship propulsion system fueled by ammonia: Environmental and economic assessments. *J. Mar. Sci. Eng.* **2020**, *8*, 183. [CrossRef]
37. Bouman, E.; Lindstad, E.; Rialland, A.; Stromman, A. State-of-the-art technologies, measures, and potential for reducing GHG emissions from shipping—A review. *Transp. Res. Part D* **2017**, *52*, 408–421. [CrossRef]
38. Nikolaidis, P.; Poullikkas, A. A comparative overview of hydrogen production processes. *Renew. Sustain. Energy Rev.* **2017**, *67*, 597–611. [CrossRef]
39. Ashik, U.; Daud, W.; Abbas, H. Production of greenhouse gas free hydrogen by thermocatalytic decomposition of methane—A review. *Renew. Sustain. Energy Rev.* **2015**, *44*, 221–256. [CrossRef]
40. Chehade, G.; Dincer, I. Progress in green ammonia production as potential carbon-free fuel. *Fuel* **2021**, *299*, 120845. [CrossRef]
41. Pawar, N.; Heinrichs, H.; Winkler, C.; Heuser, P.; Ryberg, S.; Robinius, M.; Stolten, D. Potential of green ammonia production in India. *Int. J. Hydrogen Energy* **2021**, *46*, 27247–27267. [CrossRef]
42. Zhang, H.; Wang, L.; Van herle, J.; Marechal, F.; Desideri, U. Techno-economic comparison of green ammonia production processes. *Appl. Energy* **2020**, *259*, 114135. [CrossRef]
43. IEA, The Future of Hydrogen: Seizing Today's Opportunities (Report Prepared by the IEA for the G20, Japan). Available online: https://www.iea.org/corrections/ (accessed on 1 July 2019).
44. Brown, T. *Ammonia: Zero-Carbon Fertiliser, Fuel and Energy Store*; The Royal Society: London, UK, 2020. Available online: https://www.ammoniaenergy.org/articles/royal-society-publishes-green-ammonia-policy-briefing/ (accessed on 20 February 2020).
45. Garcia, M. Hydrogen Economy Outlook: Key Messages. BloombergNEF. Available online: https://data.bloomberglp.com/professional/sites/24/BNEF-Hydrogen-Economy-Outlook-Key-Messages-30-Mar-2020.pdf (accessed on 30 March 2020).
46. Wijayanta, A.; Oda, T.; Purnomo, C.; Kashiwagi, T.; Aziz, M. Liquid hydrogen, methylcyclohexane, and ammonia as potential hydrogen storage: Comparison review. *Int. J. Hydrogen Energy* **2019**, *44*, 15026–15044. [CrossRef]
47. Cesaro, Z.; Ives, M.; Nayak-Luke, R.; Mason, M.; Banares-Alcantara, R. Ammonia to power: Forecasting the levelized cost of electricity from green ammonia in large-scale power plants. *Appl. Energy* **2021**, *282*, 116009. [CrossRef]
48. Rouwenhorst, K.; Van der Ham, A.; Mul, G.; Kersten, S. Islanded ammonia power systems: Technology review & conceptual process design. *Renew. Sustain. Energy Rev.* **2019**, *114*, 109339.
49. Aziz, M.; Wijayanta, A.; Nandiyanto, A. Ammonia as effective hydrogen storage: A review on production, storage and utilization. *Energies* **2020**, *13*, 3062. [CrossRef]
50. Makepeace, J.; He, T.; Weidenthaler, C.; Jensen, T.; Chang, F.; Vegge, T.; Ngene, P.; Kojima, Y.; Jongh, P.; Chen, P.; et al. Reversible ammonia-based and liquid organic hydrogen carriers for high-density hydrogen storage: Recent progress. *Int. J. Hydrogen Energy* **2019**, *44*, 7746–7767. [CrossRef]
51. Ishimoto, Y.; Voldsund, M.; Neksa, P.; Roussanaly, S.; Berstad, D.; Gardarsdottir, S. Large-scale production and transport of hydrogen from Norway to Europe and Japan: Value chain analysis and comparison of liquid hydrogen and ammonia as energy carriers. *Int. J. Hydrogen Energy* **2020**, *45*, 32865–32883. [CrossRef]
52. Hasan, M.; Mahlia, T.; Mofijur, M.; Fattah, I.; Handayani, F.; Ong, H.; Silitonga, A. A comprehensive review on the recent development of ammonia as a renewable energy carrier. *Energies* **2021**, *14*, 3732. [CrossRef]

53. Wan, Z.; Tao, Y.; Shao, J.; Zhang, Y.; You, H. Ammonia as an effective hydrogen carrier and a clean fuel for solid oxide fuel cells. *Energy Convers. Manag.* **2021**, *228*, 113729. [CrossRef]
54. Smith, C.; Hill, A.; Torrente-Murciano, L. Current and future role of Haber-Bosch ammonia in a carbon-free energy landscape. *Energy Environ. Sci.* **2020**, *13*, 331–344. [CrossRef]
55. Kobayashi, H.; Hayakawa, A.; Somarathne, K.; Okafor, E. Science and technology of ammonia combustion. *Proc. Combust. Inst.* **2019**, *37*, 109–133. [CrossRef]
56. Valera-Medina, A.; Xiao, H.; Owen-Jones, M.; David, W.; Bowen, P. Ammonia for power. *Prog. Energy Combust.* **2018**, *69*, 63–102. [CrossRef]
57. Erdemir, D.; Dincer, I. A perspective on the use of ammonia as a clean fuel: Challenges and solutions. *Int. J. Energy Res.* **2020**, *45*, 4827–4834. [CrossRef]
58. Hayakawa, A.; Arakawa, Y.; Mimoto, R.; Somarathne, K.; Kudo, T.; Kobayashi, H. Experimental investigation of stabilization and emission characteristics of ammonia/air premixed flames in a swirl combustor. *Int. J. Hydrogen Energy* **2017**, *42*, 14010–14018. [CrossRef]
59. Hayakawa, A.; Goto, T.; Mimoto, R.; Kudo, T.; Kobayashi, H. NO formation/reduction mechanisms of ammonia/air premixed flames at various equivalence ratios and pressures. *Mech. Eng. J.* **2015**, *2*, 14-00402. [CrossRef]
60. Hayakawa, A.; Goto, T.; Mimoto, R.; Arakawa, Y.; Kudo, T.; Kobayashi, H. Laminar burning velocity and Markstein length of ammonia/air premixed flames at various pressures. *Fuel* **2015**, *159*, 98–106. [CrossRef]
61. Ichimura, R.; Hadi, K.; Hashimoto, N.; Hayakawa, A.; Kobayashi, H.; Fujita, O. Extinction limits of an ammonia/air flame propagating in a turbulent field. *Fuel* **2019**, *246*, 178–186. [CrossRef]
62. Ichikawa, A.; Hayakawa, A.; Kitagawa, Y.; Somarathne, K.; Kudo, T.; Kobayashi, H. Laminar burning velocity and Markstein length of ammonia/hydrogen/air premixed flames at elevated pressures. *Int. J. Hydrogen Energy* **2015**, *40*, 9570–9578. [CrossRef]
63. Ichikawa, A.; Naito, Y.; Hayakawa, A.; Kudo, T.; Kobayashi, H. Burning velocity and flame structure of CH_4/NH_3/air turbulent premixed flames at high pressure. *Int. J. Hydrogen Energy* **2019**, *44*, 6991–6999. [CrossRef]
64. Ku, J.; Ahn, Y.; Kim, H.; Kim, Y.; Kwon, O. Propagation and emissions of premixed methane-ammonia/air flames. *Energy* **2020**, *201*, 117632. [CrossRef]
65. Lee, J.; Lee, S.; Kwon, O. Effects of ammonia substitution on hydrogen/air flame propagation and emissions. *Int. J. Hydrogen Energy* **2010**, *35*, 11332–11341. [CrossRef]
66. Joo, J.; Lee, S.; Kwon, O. Effects of ammonia substitution on combustion stability limits and NOx emission of premixed hydrogen-air flames. *Int. J. Hydrogen Energy* **2012**, *37*, 6933–6941. [CrossRef]
67. Um, D.; Joo, J.; Lee, S.; Kwon, O. Combustion stability limits and NOx emissions of nonpremixed ammonia-substituted hydrogen-air flames. *Int. J. Hydrogen Energy* **2013**, *38*, 14854–14865. [CrossRef]
68. Tang, G.; Jin, P.; Bao, Y.; Chai, W.; Zhou, L. Experimental investigation of premixed combustion limits of hydrogen and methane additives in ammonia. *Int. J. Hydrogen Energy* **2021**, *46*, 20765–20776. [CrossRef]
69. Zhang, M.; An, Z.; Wang, L.; Wei, X.; Jianayihan, B.; Wang, J.; Huang, Z.; Tan, H. The regulation effect of methane and hydrogen on the emission characteristics of ammonia/air combustion in a model combustor. *Int. J. Hydrogen Energy* **2021**, *46*, 21013–21025. [CrossRef]
70. Xiao, H.; Valera-Medina, A.; Bowen, P. Study on premixed combustion characteristics of co-firing ammonia/methane fuels. *Energy* **2017**, *140*, 125–135. [CrossRef]
71. Shu, T.; Xue, Y.; Zhou, Z.; Ren, Z. An experimental study of laminar ammonia/methane/air premixed flames using expanding spherical flames. *Fuel* **2021**, *290*, 120003. [CrossRef]
72. Zhu, X.; Khateeb, A.; Roberts, W.; Guiberti, T. Chemiluminescence signature of premixed ammonia-methane-air flames. *Combust. Flame* **2021**, *231*, 111508. [CrossRef]
73. Khateeb, A.; Guiberti, T.; Zhu, X.; Younes, M.; Jamal, A.; Roberts, W. Stability limits and exhaust NO performances of ammonia-methane-air swirl flames. *Exp. Therm. Fluid Sci.* **2020**, *114*, 110058. [CrossRef]
74. Okafor, E.; Naito, Y.; Colson, S.; Ichikawa, A.; Kudo, T.; Hayakawa, A.; Kobayashi, H. Measurement and modelling of the laminar burning velocity of methane-ammonia-air flames at high pressures using a reduced reaction mechanism. *Combust. Flame* **2019**, *204*, 162–175. [CrossRef]
75. Hashimoto, G.; Hadi, K.; Xia, Y.; Hamid, A.; Hashimoto, N.; Hayakawa, A.; Kobayashi, H.; Fujita, O. Turbulent flame propagation limits of ammonia/methane/air premixed mixture in a constant volume vessel. *Proc. Combust. Inst.* **2021**, *38*, 5171–5180. [CrossRef]
76. Li, J.; Huang, H.; Deng, L.; He, Z.; Osaka, Y.; Kobayashi, N. Effect of hydrogen addition on combustion and heat release characteristics of ammonia flame. *Energy* **2019**, *175*, 604–617. [CrossRef]
77. Lhuillier, C.; Brequigny, P.; Lamoureux, N.; Contino, F.; Mounaim-Rousselle, C. Experimental investigation on laminar burning velocities of ammonia/hydrogen/air mixtures at elevated temperatures. *Fuel* **2020**, *263*, 116653. [CrossRef]
78. Wang, N.; Huang, S.; Zhang, Z.; Li, T.; Yi, P.; Wu, D.; Chen, G. Laminar burning characteristics of ammonia/hydrogen/air mixtures with laser ignition. *Int. J. Hydrogen Energy* **2021**, in press.
79. Zhu, X.; Khateeb, A.; Guiberti, T.; Roberts, W. NO and OH* emission characteristics of very-lean to stoichiometric ammonia-hydrogen-air swirl flames. *Proc. Combust. Inst.* **2021**, *38*, 5155–5162. [CrossRef]

80. Mei, B.; Ma, S.; Zhang, Y.; Zhang, X.; Li, W.; Li, Y. Exploration on laminar flame propagation of ammonia and syngas mixtures up to 10 atm. *Combust. Flame* **2020**, *220*, 368–377. [CrossRef]
81. Chai, W.; Bao, Y.; Jin, P.; Tang, G.; Zhou, L. A review on ammonia, ammonia-hydrogen and ammonia-methane fuels. *Renew. Sustain. Energ. Rev.* **2021**, *147*, 111254. [CrossRef]
82. Wang, D.; Ji, C.; Wang, Z.; Wang, S.; Zhang, T.; Yang, J. Measurement of oxy-ammonia laminar burning velocity at normal and elevated temperatures. *Fuel* **2020**, *279*, 118425. [CrossRef]
83. Wang, S.; Elbaz, A.; Wang, Z.; Roberts, W. The effect of oxygen content on the turbulent flame speed of ammonia/oxygen/nitrogen expanding flames under elevated pressures. *Combust. Flame* **2021**, *232*, 111521. [CrossRef]
84. Xia, Y.; Hashimoto, G.; Hadi, K.; Hashimoto, N.; Hayakawa, A.; Kobayashi, H.; Fujita, O. Turbulent burning velocity of ammonia/oxygen/nitrogen premixed flame in O_2-enriched air condition. *Fuel* **2020**, *268*, 117383. [CrossRef]
85. Mei, B.; Zhang, X.; Ma, S.; Cui, M.; Guo, H.; Cao, Z.; Li, Y. Experimental and kinetic modeling investigation on the laminar flame propagation of ammonia under oxygen enrichment and elevated pressure conditions. *Combust. Flame* **2019**, *210*, 236–246. [CrossRef]
86. Shrestha, K.; Lhuillier, C.; Barbosa, A.; Brequigny, P.; Contino, F.; Mounaim-Rousselle, C.; Seidel, L.; Mauss, F. An experimental and modeling study of ammonia with enriched oxygen content and ammonia/hydrogen laminar flame speed at elevated pressure and temperature. *Proc. Combust. Inst.* **2021**, *38*, 2163–2174. [CrossRef]
87. Li, J.; Huang, H.; Kobayashi, N.; He, Z.; Osaka, Y.; Zeng, T. Numerical study on effect of oxygen content in combustion air on ammonia combustion. *Energy* **2015**, *93*, 2053–2068. [CrossRef]
88. Jing, Q.; Huang, J.; Liu, Q.; Wang, D.; Chen, X.; Wang, Z.; Liu, C. The flame propagation characteristics and detonation parameters of ammonia/oxygen in a large-scale horizontal tube: As a carbon-free fuel and hydrogen-energy carrier. *Int. J. Hydrogen Energy* **2021**, *46*, 19158–19170. [CrossRef]
89. Liu, Q.; Chen, X.; Huang, J.; Shen, Y.; Zhang, Y.; Liu, Z. The characteristics of flame propagation in ammonia/oxygen mixtures. *J. Hazard. Mater.* **2019**, *363*, 187–196. [CrossRef] [PubMed]
90. Choe, J.; Sun, W.; Ombrello, T.; Carter, C. Plasma assisted ammonia combustion: Simultaneous NOx reduction and flame enhancement. *Combust. Flame* **2021**, *228*, 430–432. [CrossRef]
91. Liao, Y.; Zhao, X. Plasma-assisted stabilization of lifted non-premixed jet flames. *Energy Fuels* **2018**, *32*, 3967–3974. [CrossRef]
92. Ombrello, T.; Won, S.; Ju, Y. Lifted flame speed enhancement by plasma excitation of oxygen. In Proceedings of the 47th AIAA Aerospace Sciences Meeting Including the New Horizons Forum and Aerospace Exposition, Orlando, FL, USA, 5–8 January 2009.
93. Kim, W.; Mungal, M.; Cappelli, M. Flame stabilization using a plasma discharge in a lifted jet flame. In Proceedings of the 43rd AIAA Aerospace Sciences Meeting and Exhibit, Reno, NV, USA, 10–13 January 2005.
94. Tagliante, F.; Malbec, L.; Bruneaux, G.; Pickett, L.; Angelberger, C. Experimental study of the stabilization mechanism of a lifted diesel-type flame using combined optical diagnostics and laser-induced plasma ignition. *Combust. Flame* **2018**, *197*, 215–226. [CrossRef]
95. Giorgi, M.; Ficarella, A.; Fontanarosa, D.; Pescini, E.; Suma, A. Investigation of the effects of plasma discharge on methane decomposition for combustion enhancement of a lean flame. *Energies* **2020**, *13*, 1452. [CrossRef]
96. Kong, C.; Li, Z.; Alden, M.; Ehn, A. Stabilization of a turbulent premixed flame by a plasma filament. *Combust. Flame* **2019**, *208*, 79–85. [CrossRef]
97. Valera-Medina, A.; Gutesa, M.; Xiao, H.; Pugh, D.; Giles, A.; Goktepe, B.; Marsh, R.; Bowen, P. Premixed ammonia/hydrogen swirl combustion under rich fuel conditions for gas turbines operation. *Int. J. Hydrogen Energy* **2019**, *44*, 8615–8626. [CrossRef]
98. Valera-Medina, A.; Marsh, R.; Runyon, J.; Pugh, D.; Beasley, P.; Hughes, T.; Bowen, P. Ammonia-methane combustion in tangential swirl burners for gas turbine power generation. *Appl. Energy* **2017**, *185*, 1362–1371. [CrossRef]
99. Mashruk, S.; Xiao, H.; Valera-Medina, A. Rich-quench-lean model comparison for the clean use of humidified ammonia/hydrogen combustion systems. *Int. J. Hydrogen Energy* **2021**, *46*, 4472–4484. [CrossRef]
100. Bozo, M.; Vigueras-Zuniga, M.; Buffi, M.; Seljak, T.; Valera-Medina, A. Fuel rich ammonia-hydrogen injection for humidified gas turbines. *Appl. Energy* **2019**, *251*, 113334. [CrossRef]
101. Iki, N.; Kurata, O.; Matsunuma, T.; Inoue, T.; Suzuki, M.; Tsujimura, T.; Furutani, H.; Kobayashi, H.; Hayakawa, A.; Arakawa, Y.; et al. Micro gas turbine firing ammonia. In Proceedings of the 12th Annual NH3 Fuel Conference, Chicago, IL, USA, 20–23 September 2015.
102. Iki, N.; Kurata, O.; Matsunuma, T.; Inoue, T.; Tsujimura, T.; Furutani, H.; Kobayashi, H.; Hayakawa, A.; Arakawa, Y.; Ichikawa, A. Micro gas turbine firing ammonia. In Proceedings of the ASME Turbo Expo 2016: Turbomachinery Technical Conference and Exposition, Seoul, Korea, 13–17 June 2016.
103. Iki, N.; Kurata, O.; Matsunuma, T.; Inoue, T.; Tsujimura, T.; Furutani, H.; Kobayashi, H.; Hayakawa, A. Operation and flame observation of micro gas turbine firing ammonia. In Proceedings of the ASME Turbo Expo 2017: Turbomachinery Technical Conference and Exposition, Charlotte, NC, USA, 26–30 June 2017.
104. Iki, N.; Kurata, O.; Matsunuma, T.; Inoue, T.; Tsujimura, T.; Furutani, H.; Kobayashi, H.; Hayakawa, A.; Okafor, E. NOx reduction in a swirl combustor firing ammonia for a micro gas turbine. In Proceedings of the ASME Turbo Expo 2018: Turbomachinery Technical Conference and Exposition, Oslo, Norway, 11–15 June 2018.
105. Okafor, E.; Somarathne, K.; Hayakawa, A.; Kudo, T.; Kurata, O.; Iki, N.; Kobayashi, H. Toward the development of an efficient low-NOx ammonia combustor for a micro gas turbine. *Proc. Combust. Inst.* **2019**, *37*, 4597–4606. [CrossRef]

106. Okafor, E.; Somarathne, K.; Ratthanan, R.; Hayakawa, A.; Kudo, T.; Kurata, O.; Iki, N.; Tsujimura, T.; Furutani, H.; Kobayashi, H. Control of NOx and other emissions in micro gas turbine combustors fuelled with mixtures of methane and ammonia. *Combust. Flame* **2020**, *211*, 406–416. [CrossRef]
107. Okafor, E.; Kurata, O.; Yamashita, H.; Inoue, T.; Tsujimura, T.; Iki, N.; Hayakawa, A.; Ito, S.; Uchida, M.; Kobayashi, H. Liquid ammonia spray combustion in two-stage micro gas turbine combustors at 0.25 MPa; Relevance of combustion enhancement to flame stability and NOx control. *Appl. Energy Combust. Sci.* **2021**, *7*, 100038.
108. Ito, S.; Uchida, M.; Suda, T.; Fujimori, T. Development of ammonia gas turbine co-generation technology. *IHI Eng. Rev.* **2020**, *53*, 1–6.
109. Uchida, M.; Ito, S.; Suda, T.; Fujimori, T. Performance of ammonia/natural gas co-fired gas turbine with two-stage combustor. In Proceedings of the AIChE annual meeting, Orlando, FL, USA, 10–15 November 2019.
110. IHI Becomes World's First to Attain 70% Liquid Ammonia Co-Firing Ratio on 2000-Kilowatt-Class Gas Turbine. Available online: https://www.ihi.co.jp/en/all_news/2020/resources_energy_environment/1197060_2032.html (accessed on 9 July 2021).
111. Mitsubishi Power Commences Development of World's First Ammonia-Fired 40 MW Class Gas Turbine System–Targets to Expand Lineup of Carbon-Free Power Generation Options, with Commercialization around 2025. Available online: https://power.mhi.com/news/20210301.html (accessed on 9 July 2021).
112. GE and IHI Sign Agreement to Develop Ammonia Fuels Roadmap across Asia. Available online: https://www.ge.com/news/press-releases/ge-and-ihi-sign-agreement-to-develop-ammonia-fuels-roadmap-across-asia (accessed on 9 July 2021).
113. Xia, Y.; Hadi, K.; Hashimoto, G.; Hashimoto, N.; Fujita, O. Effect of ammonia/oxygen/nitrogen equivalence ratio on spherical turbulent flame propagation of pulverized coal/ammonia co-combustion. *Proc. Combust. Inst.* **2021**, *38*, 4043–4052. [CrossRef]
114. Hadi, K.; Ichimura, R.; Hashimoto, G.; Xia, Y.; Hashimoto, N.; Fujita, O. Effect of fuel ratio of coal on the turbulent flame speed of ammonia/coal particle cloud co-combustion at atmospheric pressure. *Proc. Combust. Inst.* **2021**, *38*, 4131–4139. [CrossRef]
115. Yamamoto, A.; Kimoto, M.; Ozawa, Y.; Hara, S. Basic co-firing characteristics of ammonia with pulverized coal in a single burner test furnace. In Proceedings of the 15th Annual NH_3 Fuel Conference, Pittsburgh, PA, USA, 31 October–1 November 2018.
116. Ito, T.; Ishii, H.; Zhang, J.; Ishihara, S.; Suda, T. New technology of the ammonia co-firing with pulverized coal to reduce the NOx emission. In Proceedings of the 16th Annual NH_3 Fuel Conference, Orlando, FL, USA, 10–15 November 2019.
117. Nakamura, H.; Shindo, M. Effects of radiation heat loss on laminar premixed ammonia/air flames. *Proc. Combust. Inst.* **2019**, *37*, 1741–1748. [CrossRef]
118. Yoshizaki, T. Test of the co-firing of ammonia and coal at Mizushima power station. *J. Combust. Jpn.* **2019**, *61*, 309–312.
119. JERA and IHI to Start a Demonstration Project Related to Ammonia Co-Firing at a Large-Scale Commercial Coal-Fired Power Plant. Available online: https://www.jera.co.jp/english/information/20210524_677 (accessed on 9 July 2021).
120. Beer, J.; Chigier, N. *Combustion Aerodynamics*; John Wiley & Sons, Inc.: New York, NY, USA, 1972.
121. Kim, Y.; Lee, D.; Kim, Y. Experimental study on combustion instability and attenuation characteristics in the lab-scale gas turbine combustor with a sponge-like porous medium. *J. Mech. Sci. Technol.* **2018**, *32*, 1879–1887. [CrossRef]
122. Lee, H.; Choi, S. An observation of combustion behavior of a single coal particle entrained into hot gas flow. *Combust. Flame* **2015**, *162*, 2610–2620. [CrossRef]
123. Lee, H.; Choi, S. Motion of single pulverized coal particles in a hot gas flow field. *Combust. Flame* **2016**, *169*, 63–71. [CrossRef]
124. Lee, H.; Choi, S. Volatile flame visualization of single pulverized fuel particles. *Powder Technol.* **2018**, *333*, 353–363. [CrossRef]